NanoImpact 22 (2021) 100314

Contents lists available at ScienceDirect

NanoImpact

journal homepage: www.elsevier.com/locate/nanoimpact

Research paper

An integrated approach to testing and assessment of high aspect ratio nanomaterials and its application for grouping based on a common mesothelioma hazard

Fiona Murphy [a,*], Susan Dekkers [b], Hedwig Braakhuis [b], Lan Ma-Hock [c], Helinor Johnston [a], Gemma Janer [d], Luisana di Cristo [e], Stefania Sabella [e], Nicklas Raun Jacobsen [f], Agnes G. Oomen [b], Andrea Haase [g], Teresa Fernandes [a], Vicki Stone [a]

[a] NanoSafety Group, Heriot-Watt University, Edinburgh, UK
[b] National Institute for Public Health and the Environment (RIVM), Bilthoven, the Netherlands
[c] BASF SE, Dept. Material Physics and Dept of Experimental Toxicology & Ecology, Ludwigshafen, Germany
[d] LEITAT Technological Center, Barcelona, Spain
[e] Istituto Italiano Di Tecnologia, Genova, Italy
[f] National Research Centre for the Working Environment, Copenhagen, Denmark
[g] German Federal Institute for Risk Assessment (BfR), Department of Chemical and Product Safety, Berlin, Germany

ARTICLE INFO

Editor: Chunying Chen

Keywords:
High aspect ratio nanomaterials
Integrated approach to testing and assessment
Nanomaterial grouping

ABSTRACT

Here we describe the development of an Integrated Approach to Testing and Assessment (IATA) to support the grouping of different types (nanoforms; NFs) of High Aspect Ratio Nanomaterials (HARNs), based on their potential to cause mesothelioma. Hazards posed by the inhalation of HARNs are of particular concern as they exhibit physical characteristics similar to pathogenic asbestos fibres. The approach for grouping HARNs presented here is part of a framework to provide guidance and tools to group similar NFs and aims to reduce the need to assess toxicity on a case-by-case basis. The approach to grouping is hypothesis-driven, in which the hypothesis is based on scientific evidence linking critical physicochemical descriptors for NFs to defined fate/toxicokinetic and hazard outcomes. The HARN IATA prompts users to address relevant questions (at decision nodes; DNs) regarding the morphology, biopersistence and inflammatory potential of the HARNs under investigation to provide the necessary evidence to accept or reject the grouping hypothesis. Each DN in the IATA is addressed in a tiered manner, using data from simple *in vitro* or *in silico* methods in the lowest tier or from *in vivo* approaches in the highest tier. For these proposed methods we provide justification for the critical descriptors and thresholds that allow grouping decisions to be made. Application of the IATA allows the user to selectively identify HARNs which may pose a mesothelioma hazard, as demonstrated through a literature-based case study. By promoting the use of alternative, non-rodent approaches such as *in silico* modelling, *in vitro* and cell-free tests in the initial tiers, the IATA testing strategy streamlines information gathering at all stages of innovation through to regulatory risk assessment while reducing the ethical, time and economic burden of testing.

Abbreviations: AgNW, Silver Nanowires; CNT, Carbon Nanotube; AOP, Adverse Outcome Pathway; Dae, Aerodynamic Diameter; DN, Decision Node; HARN, High Aspect Ratio Nanomaterial; IARC, International Agency for Research on Cancer; IATA, Integrated Approach to Testing and Assessment; ISO, International Organisation for Standardization; KE, Key Event; KER, Key Event Relationship; MIE, Molecular Initiating Event; MMAD, Mass Median Aerodynamic Diameter; MPPD, Multiple Path Particle Dosimetry; MoA, Mechanism of Action; MWCNT, Multiwall Carbon Nanotube; NF, Nanoform; NiNW, Nickel Nanowire; NM, Nanomaterial; OECD, Organisation for Economic Co-operation and Development; PC, Physicochemical Characteristic; ROS, Reactive Oxygen Species; SbD, Safer-by-Design; SEM, Scanning Electron Microscopy; SOP, Standard Operating Procedure; TEM, Transmission Electron Microscopy.

* Corresponding author.
E-mail address: f.murphy@hw.ac.uk (F. Murphy).

https://doi.org/10.1016/j.impact.2021.100314
Received 2 November 2020; Received in revised form 25 February 2021; Accepted 25 March 2021
Available online 29 March 2021

1. Introduction

Grouping and read-across have evolved as important tools in the safety assessment of chemical substances including nanomaterials (NMs). Within the EU-funded project, GRACIOUS, a Framework which aims to support grouping of 'similar' nanoforms (NFs)(Commission, E, 2018) of NMs is being developed. Grouping NFs which present similar and therefore predictable fate or hazard after exposure will reduce the burden of testing individual NFs by allowing read-across of hazard data from data rich 'source' materials to 'targets' which lack data (Stone et al., 2020).

Formation of a group requires the properties of the grouped substances to be similar or follow a consistent trend. For chemical substances grouping is typically based on evidence of common chemical structures including functional groups, common precursors or common breakdown products (European Chemicals Agency, 2008). For NMs, grouping may involve different NFs (and potentially non-nanoforms) of one chemical substance. Compared to chemicals, NM grouping requires evidence of similarity in a more diverse set of physicochemical (PC) parameters with known relevance for human uptake, toxicokinetics and hazard, or environmental fate and ecotoxicity. Key intrinsic material characteristics include chemical composition, impurities and surface functionalization in addition to particle size, shape and surface area (European Chemicals Agency, 2019a). Similarity in extrinsic or system-dependent properties, defined by the surroundings in which the NF is placed (*e.g.* dissolution rate in biological media, surface reactivity and dispersibility), is also required to support grouping (Park et al., 2018). Incorporating these concepts, a number of 'pre-defined' grouping hypotheses have been generated by the GRACIOUS consortium, based on well-defined toxicokinetic pathways or mechanisms of action (MoA) to allow the user to quickly recognize a potential hazard which may be applicable to the NFs under investigation. Both intrinsic and extrinsic PC characteristics are considered by the GRACIOUS hypotheses to allow grouping of exposure-relevant material.

To assess the suitability of a GRACIOUS pre-defined hypothesis evidence from different sources (*e.g.* literature review, or experimental testing (*in chemico*, *in silico*, *in vitro*, and/or *in vivo*) is gathered *via* application of an Integrated Approach to Testing and Assessment (IATA) (OECD, 2017). By prioritising the collection of information relating to the descriptors identified by the hypothesis, the IATA facilitates a structured and focused comparison between NFs to allow acceptance or rejection of the grouping hypothesis.

Here we described a pre-defined hypothesis to group High Aspect Ratio Nanomaterials (HARNs) which present a similar hazard to the mesothelium after inhalation exposure. The potential inhalation hazard posed by HARNs is of particular concern due to the legacy of fibre-related pulmonary disease resulting from inhalation exposure to pathogenic asbestos fibres. Following inhalation, certain forms of asbestos fibres can elicit adverse health impacts including lung tumours, lung fibrosis (asbestosis) and mesothelioma, a tumour that arises from the mesothelial cells lining the chest wall and lungs. There is therefore an urgent need to differentiate between HARNs which may pose a fibre-related inhalation hazard from those which do not. Here we use the definition of a HARN as a 'NF with two similar external dimensions and a significantly larger third dimension (aspect ratio of 3:1 or greater) and substantially parallel sides'. (European Chemicals Agency, 2019b). However, aspect ratio is not the sole criteria governing potential pathogenicity and only a subcategory of all HARNs imbued with the additional characteristics which direct the fate and hazard of pathogenic fibres will pose a common mesothelioma hazard.

The GRACIOUS HARN hypothesis builds on the well-characterized and robust structure-activity relationship governing asbestos carcinogenicity, known as the fibre pathogenicity paradigm, which identifies width, length, rigidity and biopersistence of fibres as the critical determinants of mesothelioma development following inhalation (Donaldson et al., 2010). Here we provide the evidence base underpinning the GRACIOUS hypothesis for grouping HARNs which pose a similar mesothelioma hazard. Furthermore the use of the grouping hypothesis and application of the associated IATA is demonstrated to successfully differentiate different NFs and selectively group HARNs which pose a similar mesothelioma hazard, using multiwalled carbon nanotubes (MWCNT) as a case study.

2. The HARN hypothesis

The GRACIOUS consortium generated a template to structure the required content for generating a grouping hypothesis (Fig. 1). The template includes key considerations that influence a grouping decision, namely: 1) The purpose and context of grouping, 2) Lifecycle/Exposure and 3), Interaction between PC characteristics ('What they are'), Fate ('Where they go') and Hazard ('What they do'). The rationale underpinning the HARN hypothesis in terms of each of these main elements is briefly described below.

2.1. Purpose of grouping and implications of a grouping decision

Recognizing the purpose and context for grouping clarifies both the rationale for forming a group and the potential implications for HARNs being placed within a specified group (Stone et al., 2020). The pre-defined HARN hypothesis may be used by a variety of stakeholders who will benefit from the adoption of grouping approaches to streamline the hazard assessment of HARNs. Examples to illustrate the purposes for which the HARN hypothesis can be used are outlined in Table 1.

2.2. Lifecycle and exposure

Within the grouping hypothesis template, the relevant exposure scenario(s) are based on input from lifecycle and release. This scenario informs the route of exposure, which leads to subsequent considerations of the PC characteristics (what they are), toxicokinetics (where they go), and potential hazards (what they do) relevant for grouping (Stone et al., 2014).

Based on the history of occupational inhalation exposure driving the epidemic of asbestos-related disease (Stayner et al., 2013), it is pertinent to prioritise the occupational context for grouping HARNs. 'Lifecycle and exposure' assessment can highlight the potential processes and scenarios resulting in release and aerosolisation of HARNs during their production and incorporation into other products. The potential for inhalation exposure to HARNs has been reported in facilities that manufacture carbon nanotubes (CNTs)(Han et al., 2008; Lee et al., 2010; Maynard et al., 2004; Tsai et al., 2015) and those that incorporate CNTs into devices (Bello et al., 2009; Dahm et al., 2012; Cena and Peters, 2011). Certain processes such as bagging, maintenance of the reactor, and powder conditioning were associated with higher exposure levels in the production area, whereas increased exposure levels in the R&D area were related to handling of CNT powders (Kuijpers et al., 2016). Mesothelioma has been reported to develop in response to very low levels of exposure to pathogenic fibres therefore defining the exact level of release and exposure may not be critical for the safety assessment of HARN since even very low levels of exposure already pose a high risk (Noonan, 2017).

2.3. What they are?

To support evidence-based grouping, characterization of HARN PC properties is required to both verify that the 'target' HARNs adhere to the hypothesis and to allow comparison with other 'source' HARNs within the same group. The 'What they are' section of the hypothesis focuses on the specific PC characteristics shared between members of a group that determine the fate and hazard. The justification for the inclusion of critical PC descriptors which define the HARN hypothesis is briefly outlined below.

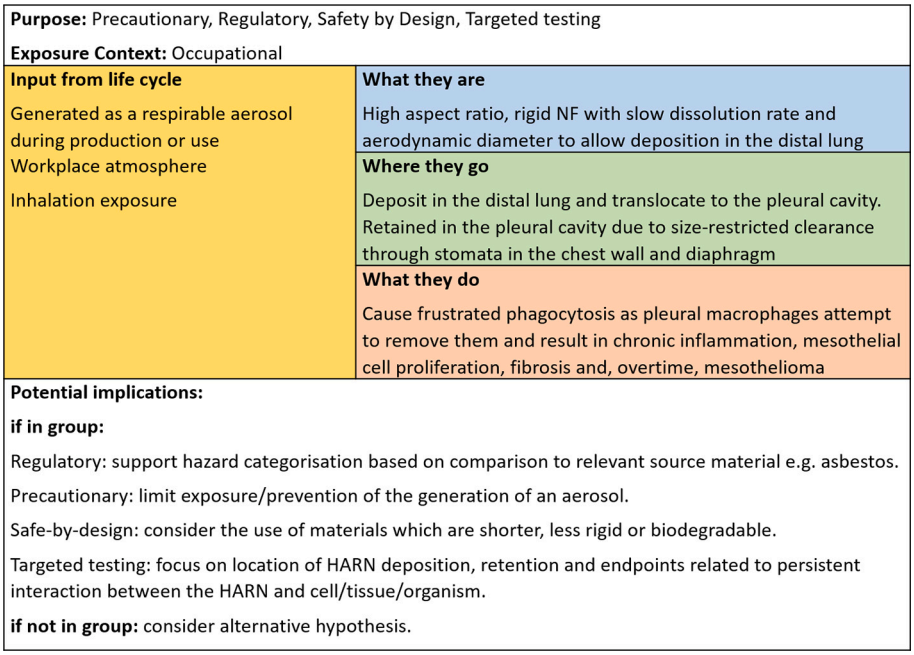

Fig. 1. Using the GRACIOUS hypothesis template to generate a grouping hypothesis for HARNs which pose a mesothelioma hazard after exposure *via* inhalation.

2.3.1. Aerodynamic diameter

Aerodynamic diameter dictates where inhaled particles will deposit along the respiratory tract (Asgharian and Yu, 1989). Inhaled fibres tend to align parallel with the airstream, therefore it is the fibre diameter rather than length which will dictate deposition along the respiratory tract. Deposition of fibres deep in the lung, beyond the ciliated airways by-passes the mucocillary escalator clearance mechanism leading to the accumulation of fibres in the distal airways of the lung.

2.3.2. Length

Fibre length has long been recognized as a critical determinant of fibre pathogenicity(Stanton et al., 1981; Davis et al., 1986; Moalli et al., 1987) as macrophages fail to effectively phagocytose fibres longer than their average diameter (ranging from 10 to 20 μm, dependent on species (Krombach et al., 1997)) leading to a state of chronic activation known as frustrated phagocytosis (Donaldson et al., 2010). The inability of macrophages to clear long fibres means that they are both more likely to be retained, and also more stimulatory and biologically active than short fibres when they make contact with cells.

HARNs including CNT (Boyles et al., 2015; Palomäki et al., 2011; Murphy et al., 2011), TiO_2 nanobelts (Hamilton et al., 2009), nickel nanowires (NiNW) and silver nanowires (AgNW)(Schinwald et al., 2012) have also been shown to hinder effective macrophage uptake leading to frustrated phagocytosis and pro-inflammatory effects *in vitro*. Length-dependent pathogenic responses *in vivo* inducing chronic inflammation (Porter et al., 2013), fibrosis and mesothelioma (Murphy et al., 2011; Chernova et al., 2017; Sakamoto et al., 2018), have similarly been reported for MWCNT.

2.3.3. Biopersistence

Biopersistence refers to both resistance to physiological clearance mechanisms (*e.g.* macrophage uptake), and resistance to chemical dissolution in biological media. Fibres composed of a material that readily undergoes chemical dissolution in the lungs (*e.g.* Synthetic Vitreous Fibres) develop weaknesses along the fibre length which eventually break producing shorter fibres (Bernstein et al., 1997). These shorter fibres can be enclosed by macrophages without the macrophage becoming activated, so the macrophage can move out of the lung with its short fibre burden. Conversely, biopersistent fibres will inhibit macrophage motility leading to a build-up of dose in the target tissue over time.

2.3.4. Rigidity

Fibre rigidity, the ability of an elongated particle to maintain its shape, without damage, when subject to mechanical forces, has recently been postulated as a fourth critical parameter dictating fibre pathogenicity in addition to diameter, length and biopersistence (Kane et al., 2018). Flexural rigidity governs whether a fibre can be buckled by compressive forces, for example, during the active process of phagocytosis by macrophages and therefore can dictate whether a fibre can be effectively cleared or conversely induce frustrated phagocytosis (Fortini et al., 2020). Rigid HARN have been shown to be more cytotoxic to macrophages and inhibit effective macrophage fibre uptake clearance, while non-rigid HARN are more easily cleared by macrophages (Zhu et al., 2016; Lehmann et al., 2019; Lee et al., 2018; Duke et al., 2017).

In addition to flexing potential, rigidity may contribute to the agglomeration state. For example, highly curled, non-rigid fibres have the propensity to form tangled agglomerates. Despite long length and high aspect ratio on an individual fibre basis, as agglomerates such HARN behave *in vivo* more like granular particles than fibres (Lee et al., 2018; Duke et al., 2017). Despite not adhering to the fibre hazard paradigm inhalation exposure to non-rigid HARN may result in toxic effects driven by alternative mechanisms of action driven for example by surface reactivity or lung overload (Saleh et al., 2020; Ma-Hock et al., 2009; Muller et al., 2008). Non-rigid HARN should therefore not be automatically considered non-hazardous but rather assessed *via* alternative toxicity hypotheses.

Intrinsic PC characteristics such as fibre length and diameter as well as system-dependent factors such as rigidity and biopersistence, directly govern the deposition and retention of fibres at the target tissues of the distal lung and serosal cavities (pleural and peritoneal). 'What they are' therefore directly impacts on 'Where they go'.

2.4. Where they go?

2.4.1. Deposition in the lung and translocation to the pleural cavity

A number of routes by which fibres translocate from the lung to the pleural cavity have been proposed (Miserocchi et al., 2008), however

Table 1
Purposes of grouping HARN.

	Implication of grouping	Example of use for HARN
Regulatory	Streamlined risk assessment of similar NFs. When compiling dossiers for regulatory purposes (*e.g.* REACH registration dossiers), grouping can be used to fill data gaps for a substance using data available on similar substances instead of conducting particular tests. This includes the possibility to apply read-across (European Chemicals Agency, 2017).	Sufficient evidence of similarity between group members may be used to support the adoption of a hazard categorization across the group in lieu of case-by-case *in vivo* testing for mesothelioma development of each group member. If the hypothesis is rejected then the user may discount mesothelioma as the critical effect in a hazard evaluation of the HARN excluded from the group.
Safe(r) by Design	Rapid and cost-effective decision making during product development of novel NFs or nano-enabled products.	To support Safe(r)-by-Design (SbD) innovation a user may wish to quickly assess whether a HARN has the potential to align or 'group' with other pathogenic fibres or HARNs shown to cause mesothelioma *in vivo* which will impact decision making regarding the continuation of the development of the product.
Precautionary	Identify adequate risk management measures for all group members during NF development or use based on information on group members for which such measures are already established.	Grouping may promote the adoption of precautionary measures for materials on which limited hazard data is available. Occupational exposure levels (OEL) or hygiene controls based on data for one data-rich group member may be adopted across the group if sufficient similarity between members can be demonstrated. For the HARNs which adhere to the grouping hypothesis, inhalation exposure would need to be prevented (or limited below the OELs for asbestos fibres) by preventing (or drastically limiting) the generation of aerosols (throughout the whole life cycle of the HARNs).

the predominant route has not been identified. Therefore, the fibre characteristics which impact on translocation are not known.

Although no studies have yet reported the presence of any engineered HARN in the pleural cavity of humans/exposed workers, biodistribution studies in rodents with CNTs have observed pleural penetration after inhalation exposure (Ryman-Rasmussen et al., 2009; Mercer et al., 2013a), and confirmed translocation to the pleural cavity (Mercer et al., 2013b; Kasai et al., 2015). A number of approaches have been utilized to identify CNT in the pleural cavity in rodent models *e.g.* by light microscopy (Murphy et al., 2012a), and enhanced dark-field microscopy (Mercer et al., 2013a) of chest wall and diaphragm tissue. Lysates from pleural lavage cell pellets have been used to quantify the translocation of MWCNT after inhalation exposure (Kasai et al., 2016). Importantly in existing studies only single fibres or discreet fibre-like bundles were identified on the parietal pleura after inhalation (Mercer et al., 2013a; Mercer et al., 2013b; Kasai et al., 2016), suggesting that the agglomerate state of fibres may affect the ability of a material to translocate to the pleural cavity.

2.4.2. *Size-restricted clearance from the pleural cavity*

Clearance of particles from the peritoneal and pleural cavities is either *via* passive drainage through stomata or pores in the mesothelial lining which connect to the lymphatic system, or *via* active removal by the resident macrophages. Both processes are size-restricted with the diameter of the stomata between 3 and 10 μm and the size limit for pleural macrophage phagocytosis approximately 15 μm (Donaldson et al., 2010; Moalli et al., 1987). It has been reported that intraperitoneal injections of short amosite asbestos (1.7% $>$ 5 μm) produced only 1 mesothelioma among 24 rats (after 837 days), while long amosite (30% $>$ 5 μm) produced 20 mesotheliomas among 21 rats (Davis et al., 1986) suggesting fibres shorter than 5 μm appear to be ineffective at inducing mesothelioma. Panels of MWCNT, NiNW and AgNW have been used to demonstrate length dependent pro-inflammatory and pro-fibrotic responses after injection directly into the peritoneal or pleural cavity. These effects were attributed to size-restricted clearance mechanisms through the stomata (Murphy et al., 2011; Schinwald et al., 2012; Poland et al., 2008). For example, Schinwald et al. (2012) confirmed a threshold of 5 μm for fibre retention in the pleural cavity, utilising a panel of AgNW with tight length cut-offs (Schinwald et al., 2012). The impact of size-restricted clearance mechanisms in the development of mesothelioma is further supported by the lack of response to short CNT (~1 μm) injected into the peritoneal cavity as the dose was rapidly cleared (Muller et al., 2009).

2.5. *What they do?*

'What they do' addresses interactions between HARNs and the target cells and tissue underlying the development of disease (mesothelioma). Furthermore 'What they do' frames the mechanistic similarity between putative group members in the activation of relevant biological responses leading to disease.

2.5.1. *Frustrated phagocytosis- NALP3 inflammasome activation*

Frustrated phagocytosis describes a phenomenon whereby macrophages are unable to completely engulf long fibres, leading to either piercing or failed closure of the macrophage cell membrane. Frustrated phagocytosis not only inhibits macrophage motility preventing clearance but leads to activation of pro-inflammatory signalling, release of cell contents, reactive oxygen species (ROS) generation and cell death, causing local tissue damage and propagating an inflammatory reaction (Mossman and Churg, 1998). It is suggested as a common mechanism of fibre toxicity to explain length-dependent pathogenicity regardless of material chemical composition. In addition to inducing acute inflammation that accompanies early injury and attempted clearance of asbestos fibres, sustained activation of immune cells by biopersistent fibres leads to the development of a chronic inflammatory response, which is considered to play a key role in the pathogenesis of fibre-related disease (Chernova et al., 2017).

Activation of the NALP3 pathway leading to interleukin-1 beta (IL-1β) release is a key feature of cells undergoing frustrated phagocytosis (Wang et al., 2017). The NALP3 inflammasome can be activated *via* disruption to the lysosome and release of the lysosomal contents into the cell. Lysosomal membrane damage in macrophages leads to release of cathepsin B from the lysosome, that activates caspase-1, resulting in activation of the NALP3 inflammasome in the cytoplasm (Sayan and Mossman, 2016). Inflammasome activation can trigger release of potent proinflammatory mediators, IL-1β and IL-18 (Broz and Dixit, 2016). Evidence for the role of chronic inflammation triggered by IL-1β signalling was reported in a murine peritoneal model of mesothelioma induced by asbestos fibres. Development of malignant mesothelioma was delayed in mice lacking a component of the NALP3 inflammasome complex or following treatment with anakinra, an inhibitor of the IL-1 receptor (Kadariya et al., 2016).

Frustrated phagocytosis is believed to be caused by fibres with a length greater than the diameter of a macrophage (10-20 μm^{24}), however the mechanism of NALP3 activation *via* lysosomal disruption may require a much shorter threshold length as has been demonstrated by studies with cerium dioxide (CeO_2) NW and AgNW (Ji et al., 2012; Schinwald and Donaldson, 2012). This therefore suggests that some

fibres can appear fully bound by the cell plasma membrane but cause lysosomal disruption within the cell and stimulate a pro-inflammatory response.

2.5.2. Chronic inflammation- link to adverse outcome pathways (AOP)

To support the acceptance of a grouping hypothesis and subsequent formation of a group, evidence is required that the group members will behave in a similar or predictable manner, leading to the development of a disease. An Adverse Outcome Pathway (AOP) is a model that identifies the sequence of molecular and cellular events required to produce a toxic effect when an organism is exposed to a substance (Villeneuve et al., 2014). The AOP connecting molecular initiating events (MIE) and adverse outcomes (AO) are defined by key events (KEs) which represent measurable biological changes, and key event relationships (KERs) between the KEs (Villeneuve et al., 2014). Two AOPs are currently under development which identify the relevant KEs in the pathway to mesothelioma development. AOP303 cites frustrated phagocytosis as a MIE in the development of lung cancer (Halappanavar et al., 2020). Contrary to well-defined MIEs for chemicals such as ligand-receptor binding or protein modification, the MIEs responsible for triggering NM-induced toxicity are vague and lack specificity often presenting as mechanical damage to cellular organelles (Gerloff et al., 2017). This broader definition of a MIE necessitated by the physical nature of NMs which includes the damaging physical interactions between macrophages and HARN exemplified by the process of 'frustrated phagocytosis'. Following frustrated phagocytosis, increased secretion of pro-inflammatory mediators (cytokines) (KE1), leads to an influx of leukocytes into lungs (KE2) and increased reactive oxygen species (ROS) generation (KE3). A sustained inflammatory response to biopersistent fibres generates a pro-tumorigenic environment characterized by oxidative stress leading to DNA damage and mutation (KE4) and increased cell proliferation (KE5). AOP171 identifies the chronic cycle of cytotoxicity and regeneration of mesothelial cells in a microenvironment of chronic inflammation and oxidative stress as the KEs driving mesothelioma formation, although for this AOP no MIE is specified (www.aopwiki.org). We propose the MIE and KEs identified in AOP303 linking frustrated phagocytosis to lung tumour formation can be integrated with the evidence base defining the KEs underlying the development of mesothelioma in AOP171 to demonstrate HARNs within a group are operating *via* the same MoA leading to mesothelioma development (Fig. 2).

3. GRACIOUS HARN IATA

The HARN mesothelioma grouping hypothesis and IATA form part of the larger GRACIOUS Framework for grouping and read-across (Stone et al., 2020). Entry to the Framework requires the end user to input basic information on the intrinsic PC characteristics (measured or estimated) of the target NFs which, combined with the purpose for grouping and relevant use/exposure scenarios will allow selection of applicable 'pre-defined' grouping hypotheses. Scenarios with the potential to release HARN into the air will short-list grouping hypotheses related to the inhalation route of exposure and basic PC characterization which identifies 'elongated' shape will prioritise the HARN hypothesis as potentially relevant for grouping.

The HARN IATA, presented in a decision tree format, logically follows the fate of the HARN from the initial inhalation exposure to the interactions with resident cells at the mesothelium leading to pathogenesis. The IATAs consist of a series of Decision Nodes (DNs) which gather the critical information required to selectively distinguish HARNs which may pose a mesothelioma hazard. Importantly the information required to satisfy each of the DNs in the IATA can be taken from existing data in the literature if the quality is considered sufficient, and so decision making does not necessarily rely on the generation of new data. However if the generation of new data is required each DN incorporates a tiered testing strategy based on the most appropriate test methods currently available for each endpoint, including validated standard operating protocols (SOPs) such as ISO protocols and OECD test guidelines where available. The tiered approach to testing, ranges from acellular or simple *in vitro* screening assays to more complex *in vitro* models and finally *in vivo* models. 'Simple' generally applies to an *in vitro* model where one cell type (cell-line or primary) is exposed to HARNs for a short period of time in submerged culture conditions and acute responses measured (*e.g.* 24 h cytotoxicity study). 'Complex' *in vitro* models are more physiologically relevant models which may use

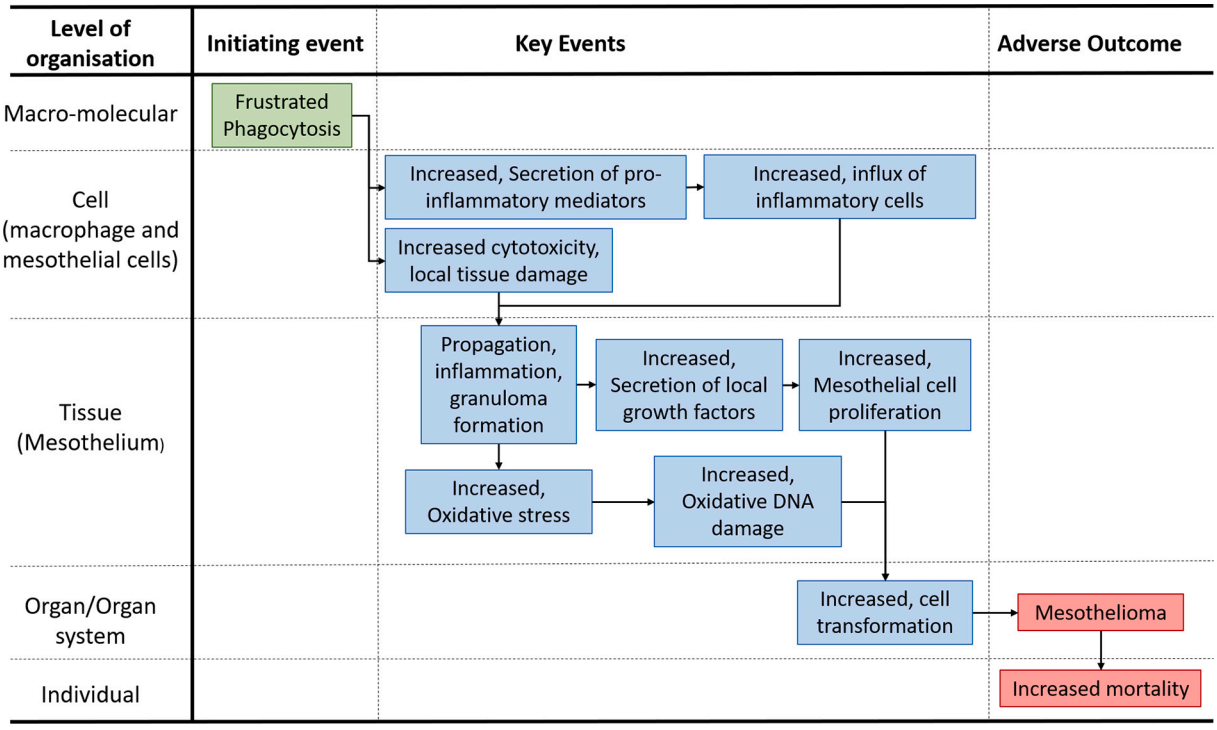

Fig. 2. Proposed AOP from frustrated phagocytosis to mesothelioma development; integration of AOPs (303 and 171).

multiple cells types in co-culture or microtissue, repeat exposures or exposures of longer durations to assess more chronic responses (Sanchez et al., 2011; Chortarea et al., 2018; Kabadi et al., 2019). Complex *in vitro* models may be used to support the basis of a group by providing more mechanistic evidence underlying a hazard prior to escalation to *in vivo* assays. The tiers chosen reflects the level of confidence required in the substantiation of the grouping hypothesis, which is dependent on the initial purpose for grouping and the associated level of uncertainty considered acceptable for the user's needs. The IATA tailored to test the applicability of the HARN hypothesis for mesothelioma hazard is outlined in Fig. 3, and the methods recommended to address each DN described in the tiered testing strategy in Table 2.

3.1. HARN mesothelioma IATA decision nodes (DN)

3.1.1. Can the HARN deposit in the distal lung?

As the mechanism of translocation from the alveolar space to the pleural cavity is not well understood there is no clear relationship between the level of deposition in the distal lung and the development of mesothelioma. Therefore if the NF meets the criteria for potential deposition in the distal regions of the lung the worst-case scenario should be assumed *i.e.* a proportion of all HARNs which deposit in the distal lung have the potential to translocate to the pleural cavity and therefore pose a mesothelioma hazard. In order to address this DN, evidence that the NF has an aerodynamic diameter (D_{ae}) of <4 μm is required as this represents the respirable fraction of particles that reach the alveoli (d50 = 4 μm) (BSI, 1993).

Addressing this DN at Tier 1 involves estimating the D_{ae} which is dependent on the measured diameter and density of the HARN. The measured diameter can be obtained either from a dispersion of the NF powder, visualized by transmission or scanning electron microscopy (TEM, SEM) following the NanoDefine protocols (Mech et al., 2020).

The potential wide variation in fibre morphology and agglomeration status of a HARN sample may lead to a high level of uncertainty in the DN outcome when based on Tier 1 estimation of D_{ae}. Qualitative electron microscopy (EM) can provide an indication of the heterogeneity within the HARN sample *i.e.* presence of fibrous and particulate fractions and level of agglomeration. The level of heterogeneity and user needs will determine whether Tier 1 estimation of D_{ae} will prove sufficient to support the conclusion on the likelihood of deposition.

For more heterogenous samples, tier 2 measurement of the mass median aerodynamic diameter (MMAD) of the aerosolised HARN can confirm the potential for inhalation and lung deposition with a higher level of confidence. Dustiness standards combine aerosol generation and aerosol measurement (BSI, 2019), and as dustiness is a required REACH parameter (Commission, E, 2018), the MMAD of the sample may be readily available.

High levels of heterogeneity of particle morphology and agglomeration state are commonly seen within aerosols of HARNs such as MWCNTs. Since fibre-like and granular particles have different

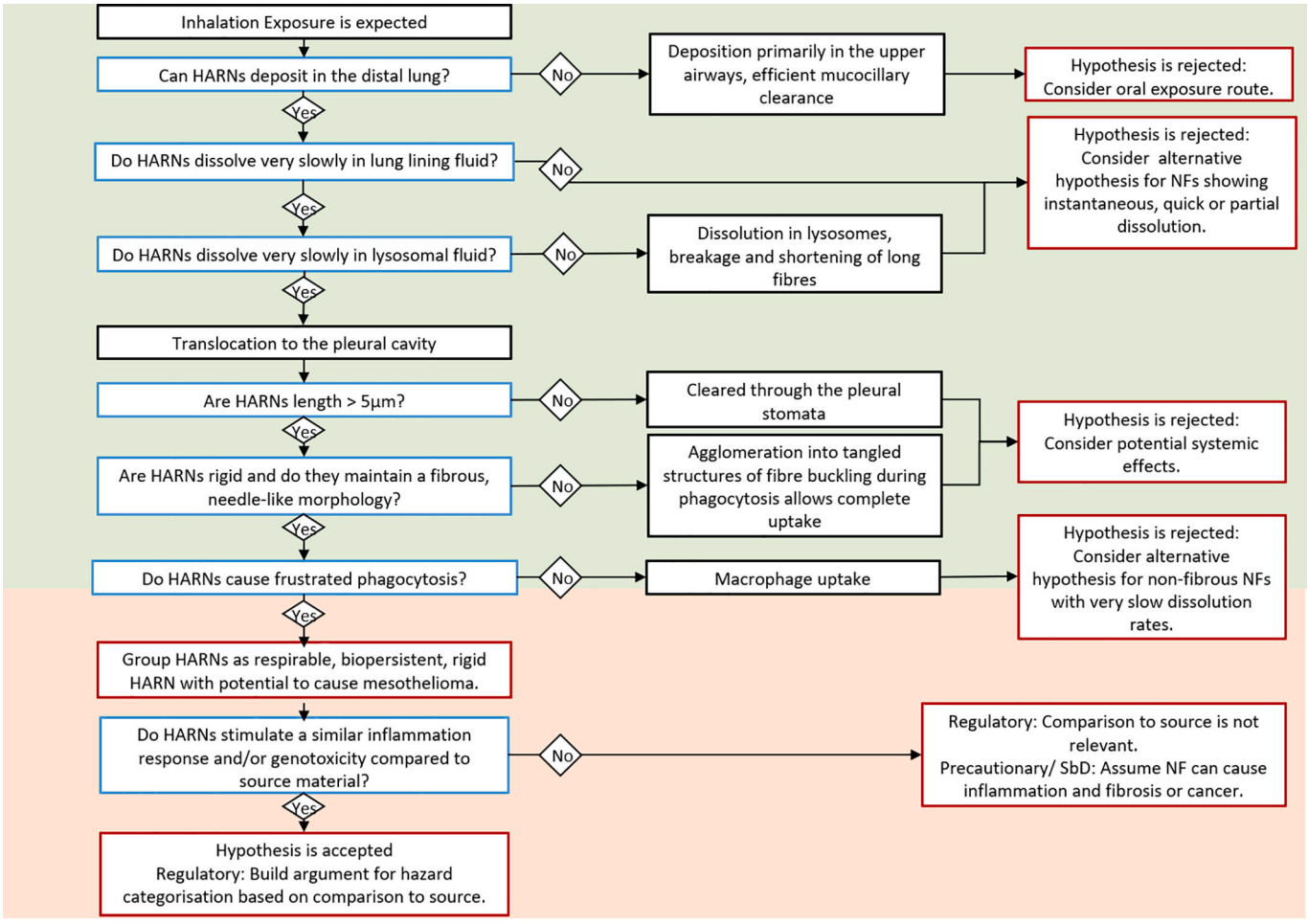

Fig. 3. HARN IATA to support the grouping hypothesis: 'Respirable, biopersistent, rigid HARNs: Following inhalation exposure and translocation of HARNs to the pleura, mesothelioma development can occur'. Blue bordered boxes are Decision Nodes, red bordered boxes are decisions, black boarded boxes are conclusions arising from addressing a decision node. The green shading relates to the 'Where they go' decision nodes and the orange shading relates to the 'What they do' decision nodes. (For interpretation of the references to colour in this figure legend, the reader is referred to the web version of this article.)

Table 2
Tiered Testing Strategy of the HARN IATA. The IATA decision nodes form the title for each column. Each tier begins with a recommendation to review the existing data sets before generating new data. The green shading relates to the 'Where they go' decision nodes and the orange shading relates to the 'What they do' decision nodes.

Can HARN deposit in the distal lung?	Does the HARN dissolve very slowly in lung lining fluid?	Does the HARN dissolve very slowly in lysosomal fluid?	Is HARN length >5μm?	Is the HARN rigid and maintain fibrous, needle-like morphology?	Does the HARN cause frustrated phagocytosis?	Does HARNs stimulate a similar inflammation response and/or genotoxicity to source material?
Tier 1						
Review existing data sets						
Estimation of D_{ae} from HARN size measurements by TEM/SEM and density measurement	Batch dissolution test in lung lining fluid (pH 7.4) or Dissolution in continuous flow system in lung lining fluid (pH 7.4)	Batch dissolution test in lysosomal fluid (pH 4.5) or Dissolution in continuous flow system in lysosomal fluid (pH4.5)	HARN size measurements by TEM/SEM	Measure diameter of HARN by TEM	Inflammasome activation: • IL-1β release • CathepsinB activity and /or release • Lysosomal Disruption	Inflammation potency: *in vitro* testing using cell lines Acute Endpoints: • Cytotoxicty • Cytokine release • Oxidative Stress • DNA damage
Tier 2						
Review existing data sets						
Measurement of MMAD by cascade impactor from an airborne dispersion of the material Lung deposition modelling: • Multiple Particle Path Deposition Model		Durability in cellular systems	HARN size measurements by TEM/SEM from an airborne dispersion of the material	HARN size measurements by TEM/SEM from an airborne dispersion of the material	*In vitro* granuloma formation	*In vitro* incubation with co-culture models of macrophages and mesothelial cells or 3D microtissue models Acute Endpoints: • Cytokine release • DNA damage Chronic: • Granuloma formation • Cell transformation
Tier 3						
Review existing data sets						
Quantification of lung burden after in vivo inhalation studies (OECD TG 412/413). Initial timepoint to measure deposition in distal lung Longer timepoint to measure biopersistence				'Biologically stiff' HARN determined experimentally by morphological assessment and size measurements after *in vitro* incubation with macrophages.	Intraperitoneal/ Intrapleural instillation: Acute Endpoint: • Inflammation, • Oxidative DNA damage Chronic: • Fibrotic lesion • Mesothelioma	

aerodynamic behaviours and distinct deposition patterns in the respiratory tract, a practical approach for interpreting the particle size analysis and MMAD from an aerosol would be to separate the particles into categories (fibrous *versus* granular) (David and Juan, 1999). The size and number of the particles in each category could then be determined and MMAD reported separately. This is in line with ECHA guidance for REACH registration, which requires a registrant to report different size distributions for different shape modalities within one material sample (European Chemicals Agency, 2019a).

For heterogenous NMs a worst-case approach should be taken, whereby all potential hazard endpoints related to the different morphologies should be considered; even a low proportion of HARNs within a sample would indicate that mesothelioma remains a potential hazard.

To assess similarity across a group of HARNs the MMAD can be utilized to facilitate comparisons between the predicted deposition patterns of HARNs as modelled by lung deposition modelling software such as the Multiple Path Particle Deposition model (Miller et al., 2016).

For HARNs above the threshold ($D_{ae} < 4$ μm) the user will exit the IATA, as the HARNs are considered unlikely to deposit in the respirable region of the lung. Deposition in the nasal cavity, throat and upper airways suggest the potential for local toxicity if the HARN is biologically reactive or alternatively potential for oral exposure as the HARN is subject to mucocilliary clearance and ingestion. Therefore an alternative hypothesis for grouping the HARN, considering alternative toxicokinetics pathway should be generated and a hypothesis-specific IATA applied.

3.1.2. Does the HARN dissolve very slowly in lung lining fluid? Does the HARN dissolve very slowly in phagolysosomal fluid?

Biopersistence takes into account dissolution and degradation in biological milieu, as well as the physical clearance of particles from the tissue by biological process such as mucociliary clearance and macrophage uptake.

Evidence of durability in physiological media is used as a predictor of biopersistence *in vivo*. This DN requires a minimum Tier 1 assessment of durability in physiologically relevant media at both neutral pH to represent the lung lining fluid, and also the low pH media which mimics the phagolysosomal fluid of macrophages. Resistance to degradation within the phagolysosome is critical for fibre biopersistence, as it will prevent the clearance of fibres by macrophage ingestion.

ISO has published guidance on the application of acellular *in vitro* tests and methodologies to assess NM durability which describes the use of both static or batch dissolution test and dynamic, continuous-flow systems (ISO, 2017). The choice of system may be dependent on, among other things, the chemical composition of the HARNs under investigation. For example, the batch dissolution assay may not be suitable for HARNs predicted to rapidly dissolve due to saturation of the medium, which will lead to inhibition of dissolution when equilibrium is reached.

The half-life ($t_{½} > 60$ days) and dissolution rate ($K_{diss} \leq 1$ ng/cm^2/h) thresholds were set to ensure only very slowly dissolving HARNs meet the DN criteria. These thresholds are based on literature from durability and biopersistence studies of mineral fibres and also recent studies of metal oxide NFs. For example, less than 1% dissolution after 56 days in phagolysosomal fluid has been reported for biopersistent crocidolite asbestos, whereas non-biopersistent MMVF22 showed 50% dissolution in the same timeframe (Maxim et al., 2002). A dissolution rate of ≤1 ng/cm^2/h has been shown to correlate with *in vivo* biopersistence; (Maxim et al., 2002) reported a K_{diss} for amosite asbestos of 1.3 ng/cm^2/h and for crocidolite asbestos of 0.15 ng/cm^2/h, both of which have been shown *in vivo* to have a half-life in the lung >100 days (Maxim et al., 2002). Biopersistent fibres or very slowly dissolving NFs should be used as

benchmark materials for inclusion in acellular assays, to confirm DN outcomes for grouping HARNs as very slowing dissolving HARNs. Electron microscopy assessment should be conducted on HARN pre and post incubation to provide qualitative evidence for the lack of transformation, such as breakage or shortening of longer fibres, due to exposure to neutral pH or low pH biological fluids.

Tier 2 recommends assays to examine durability in cellular systems which take into account a number of dynamic and physiologically relevant environments and pathways to NF degradation (Luoto et al., 1995; Nguea et al., 2008; Gualtieri et al., 2018). Progression to Tier 2 will be dependent on the user needs (higher level of confidence in durability outcome) and expert judgement (knowledge on susceptibility of different material types to enzymatic degradation). Cellular models to assess durability are not yet well standardized, however a number of studies have shown incubation with macrophages to be at least as predictive of biodurability as acellular assays for NFs (Koltermann-Jülly et al., 2018). In some cases the more physiologically relevant cellular system has been required to better understand the mechanisms of degradation (Warheit et al., 2006).

The determination of biopersistence of HARNs requires long-term *in vivo* assays (David and Juan, 1999) which are only recommended at Tier 3 of the HARN IATA. Depending on the purpose of grouping Tier 3 testing may be required to confirm acellular *in vitro* durability corresponds with an accumulation of HARN in the tissue. The updated OECD test guidelines for inhalation exposure (TG412, TG413) now require lung burdens and clearance rate to be included as recorded endpoints thereby indicating the biopersistence of the test material (OECD, 2018a; OECD, 2018b).

If the NFs do not meet the criteria to be considered biopersistent and therefore do not pose a mesothelioma hazard, the user may consider an alternative inhalation IATA to support grouping as partially or quickly dissolving HARNs. These IATAs are currently under development within GRACIOUS.

3.1.3. *Is the HARN length > 5 μm?*

Combining epidemiological data and results from *in vivo* rodent models (Davis et al., 1986; Schinwald et al., 2012; Lippmann, 1988; Stanton et al., 1977), a critical threshold length between 5 and 10 μm for mesothelioma development has been proposed (Lippmann, 2014; Boulanger et al., 2014).

HARNs generally exist as populations with a distribution of sizes, therefore a summary metric reporting median or mean fibre length is not sufficient to address this decision node. Instead, size distribution profiles should be provided. Therefore Tier 1 is based on measuring the size distribution profiles of individual HARN fibres by TEM/SEM and reporting the % fibres >5 μm. There is no clear threshold dose related to mesothelioma development, therefore it is not possible to define a proportion of fibres >5 μm that differentiates between a hazardous and non-hazardous HARN. However here we propose a pragmatic threshold of 10% of fibres counted to categorize samples as 'pathogenically long'. Whether the reported size profiles are generated from dispersions of HARNs prepared for intrinsic PC characterization (dispersed in solvent to allow visualization of individual fibres) or prepared for *in vitro/in vivo* hazard assessment (dispersed in physiological solutions with the addition of protein to reduce agglomeration) will need to be taken into account.

Tier 1 assessment of the size profiles of HARN dispersed for EM (in solvent and/or treated by ultrasonication) does not necessarily reflect the size profile of the HARN when aerosolized. Tier 2 requires the measurement of shape and size profiles from aerosolized samples and will provide confirmation that the HARN in aerosolized form will meet the threshold. The threshold to satisfy Tier 2 is set according to WHO criteria of 0.1% of particles having an aspect ratio of >3:1 and length > 5 μm(World Health Organisation, 1997) with both individual fibres and fibrous agglomerates included.

Failure to meet the DN criteria for length leads to the rejection of the hypothesis that the HARNs pose a mesothelioma hazard, as this endpoint is specifically related to long, fibrous materials. The user will be prompted to consider alternative hazard endpoints pertinent to the inhalation exposure of NFs (including spherical or granular forms) such as accumulation and toxicity in the lungs leading to fibrosis and tumour formation.

3.1.4. *Is the HARN rigid and does it maintain a fibrous, needle-like morphology?*

Diameter, alongside the elastic modulus (Youngs modulus) of a material can be used to predict fibre rigidity from the Euler Buckling theory. Fibre diameter is therefore used as an indirect indicator of rigidity of an individual HARN. A diameter of 30 nm has been set, based on evidence which suggests this is a critical threshold for fibre buckling for a number of relevant materials under compressive forces of biological process such as phagocytosis ($\sim 10^{-19}$ Nm^2) (Fortini et al., 2020; Zhu et al., 2016; Lehmann et al., 2019; Wang et al., 2019).

It is important to note that HARN such as MWCNT have the propensity to form agglomerates which may result in the formation of aligned bundles of HARNs with a fibrous structure. This may include HARN which on an individual fibre basis would be considered non-rigid but when agglomerated together will present a rigid fibre-like structure. As the secondary structure is what cells in the tissue will encounter it should be considered the biologically-relevant form potentially driving hazard. Therefore a clear distinction between the different structures of the HARN which are under investigation should be made to allow grouping of 'like with like'. Supporting EM images are needed to confirm whether the HARN are present as individual fibres, within aligned bundles or tangled agglomerates. Tier 2 methods addressing HARN rigidity and maintenance of fibrous morphology are based on assessment of an aerosolised sample of the HARN, as recommended for the fibre length DN.

Tier 3 aims to confirm whether the HARN remain rigid during the uptake and phagocytosis by macrophages. 'Biological stiffness' of aligned bundles composed of HARN, which individually may be considered flexible, can be confirmed from incubation with macrophages *in vitro*. Tier 3 is therefore a qualitative assessment of the fibre morphology of the HARN within macrophage cells *in vitro,* which may be carried out in conjunction with assays to assess inflammatory potential.

A lack of rigidity will lead to the rejection of the hypothesis that HARNs under investigation will group with HARNs that pose a mesothelioma hazard. The user will exit the IATA and be prompted to consider alternative hypotheses related to the fate and hazard of spherical NFs in the lung.

3.1.5. *Does the HARN cause frustrated phagocytosis?*

Frustrated phagocytosis has been proposed as the presumptive MIE in the mesothelioma AOP (Fig. 2). As frustrated phagocytosis is not a well-defined phenomenon which can be readily measured, this DN is based on measuring biological markers indicative of a cell undergoing frustrated phagocytosis (Palomäki et al., 2011). Tier 1 assesses acute activation of the NALP3 inflammasome *via* disruption of the lysosome. The endpoints measured include: IL-1β release, Cathepsin B release and lysosomal disruption qualitatively assessed by fluorescent microscopy or TEM. Due to the system-dependent methods to assess interactions between HARNs and cells, and the inherent biological variability in these assays, it is not possible to define a threshold whereby a HARN can be characterized as causing frustrated phagocytosis to a pathologically-relevant degree. Therefore, as well as comparing the similarity of responses between the HARNs for each endpoint, potency of HARN responses can be compared to well-characterized negative and positive benchmark controls which have been demonstrated to elicit the endpoint response under investigation, examples of appropriate benchmark controls are included in Table 3.

When introduced to an *in vitro* test system only a fraction of the applied HARN particles will come into contact with cells located at the

Table 3
Examples of appropriate benchmark materials for inclusion as controls *in vitro* assays to assess frustrated phagocytosis.

Material	Model	Endpoint	Time	Dose	Result	Ref
UICC Crocidolite asbestos	THP-1 human monomyelocytic leukemia cell line Primary murine bone marrow derived macrophages	Media supernatants were analysed for the presence of mature IL-1β by ELISA and by Western blotting.	6 h	0.05, 0.1, 0.2 mg/ml	0.2 mg/ml dose resulted in ~2.5 fold increase in IL-1β release compared to untreated cells.	Dostert et al., 2008
TiO_2 nanobelts Short <5 μm (0.8-4 μm): NB-1 Long >15 μm (15-30 μm): NB-2	Primary murine alveolar macrophages (AM)	SEM and TEM of fibre uptake CathepsinB release Fluorescent imaging of lysosomes with acridine orange IL-1β and IL-18 ELISA	Uptake assessed at 1 h Other endpoints assessed at 1, 2 4 h	100 μg/ml	NB-1 were taken up in to discrete lysosomes that were formed by the plasma membrane, NB-2 failed to produce functional lysosomes. CathepsinB activity in the AM media showed significant increases in cultures that were exposed to NB-2. IL-1β and IL-18 are significantly increased by NB-2 exposure but not NB-1 in the presence of a low concentration of the co-stimulant lipopolysaccaride (LPS).	Hamilton et al., 2009
Mitsui-7 MWCNT	THP-1 human monomyelocytic leukemia cell line	CNT uptake by light microscopy and SEM IL-1β ELISA	24 h	5 μg/cm^2	Mitui-7 caused a significant increase in IL-1β compared to untreated cells and cells exposed to short MWCNT and Printex90. Mitsui-7 appears to be protruding from the cells by light microscopy and SEM.	Murphy et al., 2012a,b
Mitsui-7 UICC Crocidolite asbestos	Human peripheral blood monocytes	NALP3 inflammasome activation IL-1β ELISA	6 h	100 μg/ml	Mitsui-7 and crocidolite asbestos activate NALP3 inflammasome *via* ROS production, CathepsinB activaiton and Src and Syk kinases leading to IL-1β secretion.	Palomaki et al., 2011

bottom of a cell culture vessel within a given timeframe. *In vitro* assessment of HARNs should therefore be accompanied by determination of the effective dose of particles that have come into contact with cells, in order to achieve meaningful dose-response assessments and to compare similarity between HARNs. A number of models and approaches for dosimetry calculations *in silico* have been published (DeLoid et al., 2015; Hinderliter et al., 2010; Liu et al., 2015; Thomas et al., 2018; Bitounis et al., 2019). As HARNs will behave differently when settling in culture from spherical particles, Price et al., 2019 have developed a simple computational particokinetics model to adapt current dosimetry models to facilitate applicability to HARNs (Price et al., 2019).

A proposed Tier 2 level assay measures the development of 3D macrophage granulomas in response to longer-term *in vitro* exposure to HARNs (Sanchez et al., 2011). To date this model has not been extensively tested or validated, and as such should only be used for targeted testing to further illuminate similarity between HARNs in terms of MoA. Evidence of granuloma formation which represents the potential development of a chronic inflammatory response to HARNs can strengthen an argument to group similar HARNs as potentially pathogenic, as the establishment of chronic inflammation is a KE in the AOP for tumour development triggered by frustrated phagocytosis (Fig. 2) (Halappanavar et al., 2020). Confirmation of a chronic response to the HARN, reflective of fibre pathogenicity *in vivo*, will also reduce uncertainty inherent in the short-term assays included in Tier 1. These assays only measure acute pro-inflammatory responses to HARNs which may resolve over time, or alternatively be triggered by alternative mechanisms unrelated to fibre morphology.

The failure to elicit a pro-inflammatory response *in vitro*, when compared to a well-characterized benchmark material which is indicative of frustrated phagocytosis, suggests that the HARN in question will be successfully engulfed and pacified by the resident macrophages and therefore will not trigger the chronic pro-inflammatory environment required for mesothelioma development. At this point the hypothesis is rejected and the user will exit the IATA.

3.2. The IATA outcome

Based on the above DNs a user can decide whether to accept or reject the grouping hypothesis. Adherence to the IATA DNs, provides support to accept the hypothesis for the provisional grouping of the NMs as respirable, biopersistent, rigid HARNs with potential to cause mesothelioma. Such an outcome may be a sufficient outcome for precautionary or SbD purposes. Regulatory purposes, such as the adoption of a hazard catergorization (*e.g.* IARC classification of carcinogenicity) across the group, will require evidence of a high degree of similarity between the HARN group members for each of the DNs described above. Defining similarity between HARNs will require extensive assessment of the literature supplemented with empirical evidence from case studies to set similarity limits. A range of methods to assess similarity have been designed and are currently being tested. For regulatory purposes, evidence of mechanistic similarity in the inflammatory potential and genotoxicity posed by the grouped HARNs should also be demonstrated. Endpoints for assessing the inflammatory and genotoxicity potential should be informed by the mesothelioma AOP (Fig. 2) to ensure the information gathered is targeted and can be interpreted in terms of disease relevance. Inflammatory potential and genotoxicity can be tested in tiers from simple *in vitro* assays using cell-lines and acute endpoints (Tier 1), to more complex and physiologically-relevant *in vitro* models incorporating multiple cell types conducted over longer exposure times (Tier 2), or if necessary Tier 3 *in vivo* models (Table 2).

4. Case study

The performance of the HARN mesothelioma IATA was evaluated using a literature case study. Only long-term studies with the potential to result in mesothelioma development were included, which to date is limited to studies conducted with MWCNT.

A literature search was conducted to identify studies assessing the mesothelioma-generating potential of MWCNT. Studies assessing the mesothelioma-potential of a single MWCNT were used to test the use of the IATA to predict mesothelioma hazard (Fig. 4A), whereas studies which included multiple MWCNTs tested whether the IATA is stringent enough to differentiate between mesothelioma-positive and mesothelioma-negative MWCNT (Fig. 4B).

Between 2008 and 2020 fourteen *in vivo* studies have assessed the potential of MWCNT to cause mesothelioma development in rodent models (Table 4). Routes of administration included direct injection into the peritoneal (8 studies) and pleural (1 study) cavities, injection into the scrotal sac (1 study), capsule implantation into a 'Kertai fold' in the

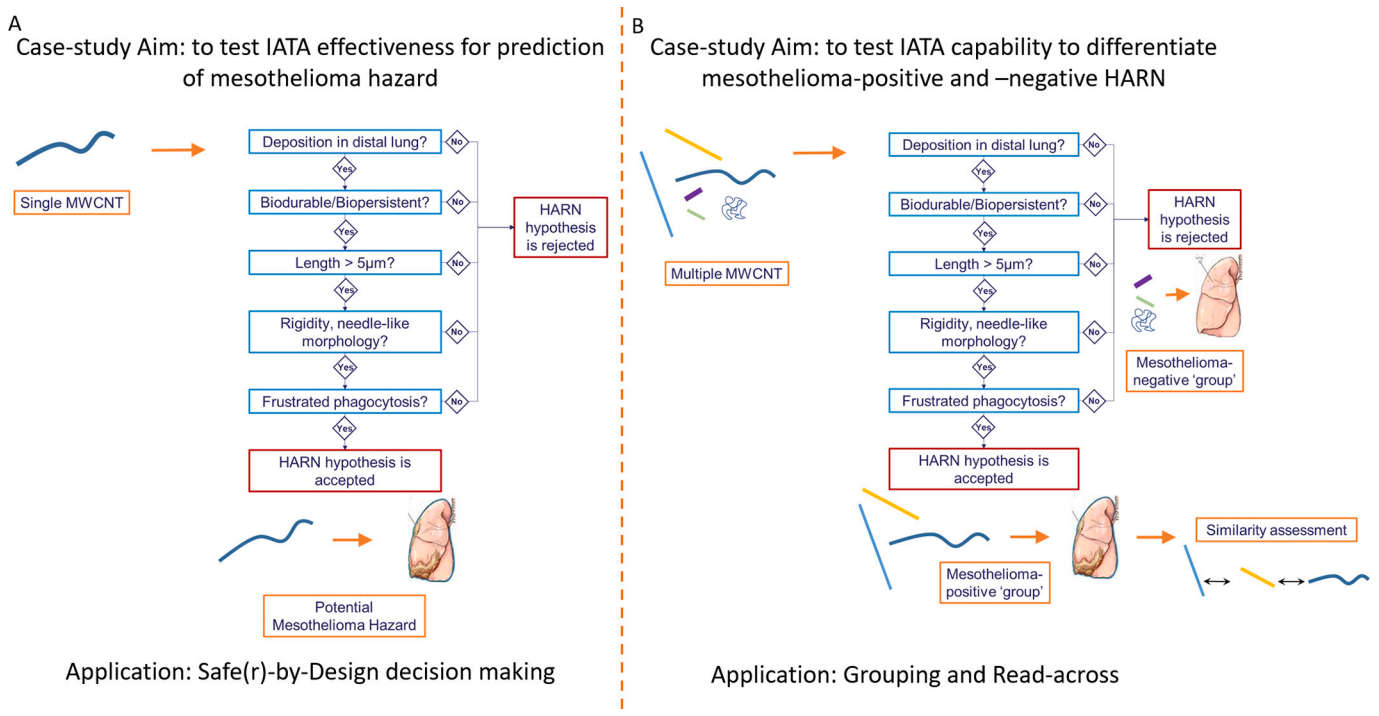

Fig. 4. Illustrative example of how studies assessing the mesothelioma-generating potential of single (A) or multiple MWCNT (B) were used to substantiate the HARN IATA.

peritoneal cavity (1 study) and into the lungs by intratracheal spraying (3 studies). Across the 14 studies published, 16 different MWCNT were assessed for their potential to induce mesothelioma development. Based on the reported mesothelioma incidence, MWCNT from each study were categorized as mesothelioma-positive (10) or mesothelioma-negative (6) (Table 4).

Information relevant to answering each DN in the HARN IATA was extracted from each study and a preliminary IATA-driven assessment of the potential to accept the grouping hypothesis for each of the MWCNTs was assessed (Table 5). The initial assessment based on the data provided within the mesothelioma studies suggests the IATA can distinguish between mesothelioma-positive and mesothelioma-negative MWCNT, however data gaps were evident. As the majority of studies directly applied the MWCNT to the mesothelium (intraperitoneal, intrapleural or intrascrotal injection), information regarding the deposition of MWCNT in the distal regions of the lung was lacking. It is not appropriate to extrapolate potential risk to inhalation exposure of HARN, as the models do not replicate a realistic inhalation exposure scenario. However, the focus of the presented IATA is to support a common mesothelioma hazard, for which the models included in the case studies are considered sufficiently predictive.

The majority of existing *in vivo* studies did not examine the interactions between the MWCNT and macrophages *in vitro*, therefore the DN evaluating the propensity of a HARN to cause frustrated phagocytosis could not be addressed by these studies. Evidence to support a 'group' of HARNs operate *via* the same MoA underlying the pathogenesis of mesothelioma development was therefore lacking.

The IATA conclusively rejected the grouping hypothesis for 6 different MWCNT, as they were not sufficiently long or rigid. None of the MWCNT rejected by the IATA caused mesothelioma formation in the rodent models tested. Therefore the IATA were sufficiently stringent to exclude 'mesothelioma-negative' MWCNT from the proposed group.

To fill identified data gaps and to reduce uncertainty, specific information from additional *in vivo* and *in vitro* studies was sought. A targeted literature search was conducted, restricted to the specific MWCNT with a defined mesothelioma outcome (positive or negative), and information relevant to each of the DNs was integrated across studies to allow progression through the IATA (Table 6). Of the 16 MWCNT categorized for mesothelioma potential, additional supporting studies for 4 mesothelioma-positive and 2 mesothelioma-negative MWCNT samples was found. Sufficient additional information to confirm the acceptance of the hypothesis for one MWCNT, Mitsui-7 was identified. Although additional information supporting the adherence of the hypothesis for the other 3 mesothelioma-positive MWCNT was collected, data gaps remained. No evidence for the rejection of the hypothesis was reported using data obtained from the additional studies suggesting the hypothesis can be provisionally accepted until further information is available. Further evidence to support the rejection of the hypothesis for the 2 mesothelioma-negative MWCNT was identified, increasing certainty in the IATA outcome.

Although largely considered to be of sufficient quality, a number of weaknesses common among the studies were identified, primarily concerning data gaps in characterization of the MWCNT *e.g.* level of impurities. Limited reporting of size distribution profiles and reliance on the use of a sole summary metric, such as mean or median length and diameter, provides an incomplete and potentially biased representation of the MWCNT size profiles.

We also assessed whether all the critical descriptors relevant for consideration of mesothelioma potential were included within the IATA. Information was collected from the literature on additional descriptors such as MWCNT purity, presence of contaminants, and surface defects, as indicated by D/G ratio measured by Raman spectroscopy (Dresselhaus et al., 2010). MWCNT were ranked high-to-low for these physicochemical descriptors and compared against the MWCNT mesothelioma potential (Table 7). No trend reflective of mesothelioma development was identified, suggesting that the HARN IATA does not need to be expanded to include such data.

5. Discussion

Here we demonstrate an evidence-based grouping approach for HARNs, whereby a grouping hypothesis is first formulated, based on

Table 4
Mesothelioma potential of MWCNT based on a review of the literature. Grey boxes: Mesothelioma-negative MWCNT (Takagi et al., 2008; Muller et al., 2005; Sakamoto et al., 2009; Varga and Szendi, 2010; Nagai et al., 2011; Takagi et al., 2012; Nagai et al., 2013; Rittinghausen et al., 2014; Huaux et al., 2016; Suzui et al., 2016; Chernova et al., 2017; Sakamoto et al., 2018; Numano et al., 2019; Abdelgied et al., 2019).

Study	MWCNT	Dose	Route of Administration	Mesothelioma Incidence
Takagi 2008	Mitsui-7	3mg/mouse (1x10^9 fibres)	Intraperitoneal	87.5% (14/16)
Muller 2009	MWCNT+	2mg/rat	Intraperitoneal	4% (2/50) (Considered spontaneous tumour due to tumour location and evidence of tumours in vehicle)
		20mg/rat		0% (0/50)
	MWCNT-	20mg/rat		6% (3/50) (Considered spontaneous tumour due to tumour location and evidence of tumours in vehicle)
Sakamoto 2009	Mitsui-7	1mg/kg (~0.25mg/rat)	Intrascrotal	86% (6/7)
Varga 2010	MWCNT	10mg/rat	Implantation to Kerati fold	0% (0/6)
Nagai 2011	NT50a (Mitsui-7)	1mg/rat	Intraperitoneal	100% (13/13)
		10mg/rat		100% (43/43)
	NT50b	10mg/rat		100% (6/6)
	NT145	1mg/rat		17% (5/29)
		10mg/rat		93% (28/30)
	NTtng1	10mg/rat		0% (0/6)
Takagi 2012	Mitsui-7	1X10^8 fibres 300µg/mouse	Intraperitoneal	95% (19/20)
		1x10^7 fibres 30µg/mouse		85% (17/20)
		1x10^6 3µg/mouse		25% (5/20)
Nagai 2013	NTtng1	10mg/rat	Intraperitoneal	0% (0/6)
Rittinghausen 2014	MWCNT A	0.48x10^9 fibres 0.2mg/rat	Intraperitoneal	98% (49/50)
		2.39X10^9 fibres 1mg/rat		90% (45/50)
	MWCNT B	0.96x10^9 fibres 0.6mg/rat		92% (46/50)
		4.80x10^9 fibres 3mg/rat		90% (45/50)
	MWCNT C	0.87x10^9 fibres 0.08mg/rat		84% (42/50)
		4.36x10^9 fibres 0.4mg/rat		94% (47/50)
	MWCNT D	1.51x10^9 fibres 0.05mg/rat		40% (20/50)
		7.54x10^9 fibres 0.25mg/rat		70% (35/50)
Huaux 2016	CNT-7	6mg/rat (2x10^9 WHO fibres/rat)	Intraperitoneal	100% (50/50)
	Short CNT-7	6mg/rat (0.36x10^9 WHO fibres)		100% (50/50)
Suzui 2016	N-CNT	1mg/rat	Intratracheal Spraying	25% (3/12)
	N-CNT Flow through fraction	1mg/rat		25% (3/12)
Chernova 2017	NTlong	0.2µg/mouse	Intrapleural	8.3% (1/12)
		0.5µg/moue		20% (1/5)
		1µg/mouse		20% (1/5)
		2.5µg/mouse		25% (1/4)
Sakamoto 2018	M-CNT (Mitsui-7)	1mg/kg (~0.25mg/rat)	Intraperitoneal	100% (12/12)
	N-CNT	1mg/kg (~0.25mg/rat)		100% (10/10)
	SD1	1mg/kg (~0.25mg/rat)		100% (14/14)
	WL	1mg/kg (~0.25mg/rat)		100% (15/15)
	SD2 (NTtng1)	1mg/kg (~0.25mg/rat)		0% (0/14)
	WS	1mg/kg (~0.25mg/rat)		7% (1/14) (Considered spontaneous tumour due to tumour location and evidence of tumour in vehicle)
	T-CNT	1mg/kg (~0.25mg/rat)		8% (1/13) (Considered spontaneous tumour due to tumour location and evidence of tumour in vehicle)
Numano 2019	Mitsui-7	1.5mg/rat	Intratracheal Spraying	95% (18/19)
Abdelgied 2019	Mitsui-7	0.5mg/rat	Intratracheal Spraying	14% (2/14)

Table 5
Summary of MWCNT compared against the HARN IATA DN criteria for published *in vivo* studies. Conclusion of DN: YES (green), UNCERTAIN (amber), NO (red) provided for each decision node. 'Not reported': information to address DN not provided in the study (grey) (Takagi et al., 2008; Muller et al., 2009; Sakamoto et al., 2009; Varga and Szendi, 2010; Nagai et al., 2011; Takagi et al., 2012; Nagai et al., 2013; Rittinghausen et al., 2014; Huaux et al., 2016; Suzui et al., 2016; Chernova et al., 2017; Sakamoto et al., 2018; Numano et al., 2019; Abdelgied et al., 2019; Morimoto et al., 2012; Oyabu et al., 2011).

Study	MWCNT	Deposition in the distal lung/ translocation to the pleural cavity	Dissolution/ Biopersistence	Fibre length >5μm	Rigid, needle-like morphology	Frustrated Phagocytosis
Takagi 2008	Mitsui-7	**DN: Not reported** Particle size or density measurements were not available to predict lung deposition	**DN: UNCERTAIN** Predicted to be biodurable based on pristine carbon chemistry.	**DN: YES (Tier 1)** 27.5% > 5μm in length	**DN: YES (Tier1)** 85% between 70-100nm	**DN: Not reported**
Muller 2009	MWCNT+	**DN: Not reported**	**DN: UNCERTAIN** Predicted to be biodurable based on pristine carbon chemistry.	**DN: NO (Tier 1)** Approx. 0.7μm Not possible to accurately measure length due to high levels of agglomeration. Size distribution not provided	**DN: NO (Tier 1)** 11.3±3.9nm TEM images of highly curled fibres: not rigid	**DN: Not reported**
	MWCNT-	**DN: Not reported**	**DN: UNCERTAIN** Predicted to be biodurable based on pristine carbon chemistry.	**DN: NO (Tier 1)** Approx. 0.7μm Not possible to accurately measure length due to high levels of agglomeration. Size distribution not provided	**DN: NO (Tier 1)** 11.3±3.9nm TEM images of highly curled fibres: not rigid	**DN: Not reported**
Sakamoto 2009	Mitsui-7	**DN: Not reported**	**DN: UNCERTAIN** Predicted to be biodurable based on pristine carbon chemistry.	**DN: Not reported** Refers to Takagi *et al* 2008[96], same MWCNT lot number	**DN: Not reported** Refers to Takagi *et al* 2008[96], same MWCNT lot number	**DN: Not reported**
Varga 2010	MWCNT	**DN: Not reported**	**DN: UNCERTAIN** Predicted to be biodurable based on pristine carbon chemistry.	**DN: NO (Tier 1)** Reported as 1-2μm. No further information on size distribution provided. No supporting images of MWCNT provided. Short length range reported would suggest the threshold of 5μm is not reached	**DN: NO (Tier 1)** 10-30nm No further information on size distribution provided. No supporting images of MWCNT provided. Maximum diameter of 30nm suggests threshold for rigidity is not reached	**DN: Not reported**
Nagai 2011	NT50a (Mitsui-7)	**DN: Not reported**	**DN: UNCERTAIN** Predicted to be biodurable based on pristine carbon chemistry.	**DN: YES (Tier 1)** Mean: 5.29±0.12μm Size distribution histogram also provided. Log normal distribution. Graph suggests 10-50% ≥ 5μm	**DN: YES (Tier1)** Mean: 49.95±0.63nm	**DN: YES (Tier1)** Dose-dependent moderate cytotoxicity to RAW264.7 after 4 days. Significant increase in IL-1β and IL-6 mRNA after 24 hours
	NT50b	**DN: Not reported**	**DN: UNCERTAIN** Predicted to be biodurable based on pristine carbon chemistry.	**DN: YES (Tier 1)** Mean: 4.6±0.1μm Size distribution histogram also provided. Log normal distribution. Graph suggests 10-50% ≥ 5μm.	**DN: YES (Tier1)** Mean: 52.4±0.72nm	**DN: Not reported** NT50b not included in in vitro assay
	NT145	**DN: Not reported**	**DN: UNCERTAIN** Predicted to be biodurable based on pristine carbon chemistry.	**DN: YES (Tier 1)** Mean: 4.34±0.08μm Size distribution histogram also provided. Log normal distribution. Graph suggests 10-50% ≥ 5μm.	**DN: YES (Tier1)** Mean: 143.5±0.5.5nm	**DN: YES (Tier1)** Dose dependent moderate cytotoxicity to RAW264.7 after 4 days. Significant increase in IL-1β and IL-6 mRNA after 24 hours
	NTtng1	**DN: Not reported**	**DN: UNCERTAIN** Predicted to be biodurable based on pristine carbon chemistry.	**DN: NO (Tier 1)** 3μm (From manufacturer) Not measured by authors due to highly tangled nature of MWCNT. Not further information on size distribution provided.	**DN: NO (Tier 1)** 15nm (From manufacturer) Non-rigid nature of MWCNT confirmed by TEM and light microscopy images of highly tangled nature of MWCNT	**DN: UNCERTAIN** No cytotoxicity to RAW264.7 macrophages after 4 days. No results reported for inflammatory markers
Takagi 2012	Mitsui-7	**DN: Not reported**	**DN: UNCERTAIN** Predicted to be biodurable based on pristine carbon chemistry.	**DN: YES (Tier 1)** 27.5% > 5μm in length	**DN: YES (Tier1)** 85% between 70-100nm	**DN: Not reported**
Nagai 2013	NTtng1	**DN: Not reported**	**DN: UNCERTAIN** Predicted to be biodurable based on pristine carbon chemistry.	**DN: NO (Tier 1)** 3μm (From manufacturer) Not measured by authors due to highly tangled nature of MWCNT. Not further information on size distribution provided.	**DN: NO (Tier 1)** 15nm (From manufacturer) Non-rigid nature of MWCNT confirmed by TEM and light microscopy images of highly tangled nature of MWCNT	**DN: Not reported**
Rittinghausen 2014	MWCNT A	**DN: Not reported**	**DN: UNCERTAIN** Predicted to be biodurable based on pristine carbon chemistry.	**DN: YES (Tier1)** Proportion of total > 5μm not reported however 3.81% > 20μm Mean: 2.72±2.29μm	**DN: YES (Tier1)** Mean: 85±1.6nm	**DN: Not reported**
	MWCNT B	**DN: Not reported**	**DN: UNCERTAIN** Predicted to be biodurable based on pristine carbon chemistry.	**DN: YES (Tier1)** Proportion of total > 5μm not reported however 9.35% > 20μm Mean: 2.13±2.46 μm	**DN: YES (Tier1)** Mean: 62±1.71nm	**DN: Not reported**

	MWCNT C	**DN: Not reported**	**DN: UNCERTAIN** Predicted to be biodurable based on pristine carbon chemistry.	**DN: YES (Tier1)** Proportion of total > 5µm not reported however 11.77% > 20µm Mean: 4.18±2.41µm	**DN: YES (Tier1)** Mean: 40±1.57nm	**DN: Not reported**
	MWCNT D	**DN: Not reported**	**DN: UNCERTAIN** Predicted to be biodurable based on pristine carbon chemistry.	**DN: YES (Tier1)** Proportion of total > 5µm not reported however 2.13% > 20µm Mean: 2.53±2.02µm	**DN: YES (Tier1)** Mean: 37±1.45nm	**DN: Not reported**
Huaux 2016	Mitsui-7	**DN: Not reported**	**DN: UNCERTAIN** Predicted to be biodurable based on pristine carbon chemistry.	**DN: YES (Tier1)** Median: 7.1µm 78% > 5µm	**DN: YES (Tier1)** 75nm	**DN: Not reported**
	Short Mitsui-7	**DN: Not reported**	**DN: UNCERTAIN** Predicted to be biodurable based on pristine carbon chemistry.	**DN: YES (Tier 1)** Median: 2.8µm 14% > 5µm	**DN: YES (Tier1)** 75nm	**DN: Not reported**
Suzui 2016	N-CNT	**DN: Not reported**	**DN: YES (Tier 3)** Lung burden reported at end of study (109 weeks) 25.4% compared to week 2 (end of interval dosing) Biopersistence half-life in vivo (Tier 3) > 100 days	**DN: YES (Tier 1)** Mean: 4.2±2.9µm Range 1-10µm 47% > 5µm	**DN: YES (Tier1)** 93.4% between 30-80nm	**DN: Not reported**
	N-CNT FTF	**DN: Not reported**	**DN: YES (Tier 3)** Lung burden reported at end of study (109 weeks) 48% compared to week 2 (end of interval dosing) Biopersistence half-life in vivo (Tier 3) > 100 days	**DN: YES (Tier 1)** Mean: 2.6±1.6µm Range 1-10µm % fibres > 5µm not reported Falls into YES category, due to wide range up to 10µm	**DN: YES (Tier1)** 93.4% between 30-80nm	**DN: Not reported**
Chernova 2017	NTlong	**DN: Not reported**	**DN: UNCERTAIN** Predicted to be biodurable based on pristine carbon chemistry.	**DN: YES (Tier1)** Proportion of fibres > 5µm not reported however 84.26% > 15µm Mean: 36µm	**DN: YES (Tier1)** Mean: 165.02 ±4.68nm	**DN: Not reported**
Sakamoto 2018	M-CNT (Mitsui-7)	**DN: Not reported**	**DN: UNCERTAIN** Predicted to be biodurable based on pristine carbon chemistry.	**DN: YES (Tier1)** Mean: 6.65µm 54% > 5µm	**DN: YES (Tier1)** Mean: 66.8nm 64% between 60-100nm	**DN: Not reported**
	N-CNT	**DN: Not reported**	**DN: UNCERTAIN** Predicted to be biodurable based on pristine carbon chemistry.	**DN: YES (Tier 1)** Mean: 5.48µm 38% > 5µm	**DN: YES (Tier1)** Mean: 59.2nm 33% between 60-100nm	**DN: Not reported**
	SD1	**DN: Not reported**	**DN: UNCERTAIN** Predicted to be biodurable based on pristine carbon chemistry.	**DN: YES (Tier 1)** Mean: 4.52µm 38% > 5µm	**DN: YES (Tier1)** Mean: 177.4nm 89% > 100nm	**DN: Not reported**
	WL	**DN: Not reported**	**DN: UNCERTAIN** Predicted to be biodurable based on pristine carbon chemistry.	**DN: YES (Tier1)** Mean: 7.31µm 59% > 5µm	**DN: YES (Tier1)** Mean 70.9nm 41% between 60-100nm	**DN: Not reported**
	SD2 (NTtng1)	**DN: Not reported**	**DN: UNCERTAIN** Predicted to be biodurable based on pristine carbon chemistry.	**DN: NO (Tier 1)** 0.5-2µm from manufacturers Not measurable by authors due to highly tangled nature	**DN: NO (Tier 1)** Mean: 44.5nm 92% between 20-50nm Supporting SEM provides evidence for lack of rigidity. Highly tangled, no needle-like fibres.	**DN: Not reported**
	WS	**DN: Not reported**	**DN: UNCERTAIN** Predicted to be biodurable based on pristine carbon chemistry.	**DN: NO (Tier 1)** 3µm from manufacturer Not measurable by authors due to highly tangled nature	**DN: NO (Tier 1)** Mean: 13.5nm 100%: 10-30nm	**DN: Not reported**
	T-CNT	**DN: Not reported**	**DN: UNCERTAIN** Predicted to be biodurable based on pristine carbon chemistry.	**DN: NO (Tier 1)** 0.732 µm from manufacturer Not measurable by authors due to highly tangled nature	**DN: NO (Tier 1)** Mean: 35.8nm 93%: 10-50nm Supporting SEM provides evidence for lack of rigidity. Highly tangled, no needle-like fibres.	**DN: Not reported**
Numano 2019	Mitsui-7	**DN: Deposition Not Addressed** **Translocation: YES (Tier 3)** MWCNT-7 fibers were observed in the mesotheliomas that developed, primarily associated with macrophages.	**DN: YES (Tier 3)** Fibres digested from the lung demonstrates the persistence of fibres > 5µm in the lung tissue after 104 weeks. Lengths are comparable to the lengths of Mit-7 reported previously suggesting no reduction of length indicative of lack of biopersistence.	**DN: YES (Tier 1)** Mean: 4.8 ± 2.8µm Median: 4.2µm From size distribution histogram provided estimate 35-40% > 5µm. *Lengths of fibres collected from the lung after digestion at the end of study.	**DN: Not reported**	**DN: Not reported**
Abdelgied 2019	Mitsui-7	**DN: Not reported**	**DN: YES (Tier 3)** Long fibres were retrieved from digested tissue at the end of the study from the lung and pleural cavity. No shortening/thinning of fibres was evident from comparison of the average lengths and diameters from the instilled suspension and the retrieved fibres.	**DN: YES (Tier1)** Mean: 5.31±3.81µm	**DN: YES (Tier1)** Mean: 75.65±20.54nm	**DN: Not reported**

Table 6
IATA outcome for each case study MWCNT after integration of supporting information from additional studies (Takagi et al., 2008; Sakamoto et al., 2009; Nagai et al., 2011; Takagi et al., 2012; Huaux et al., 2016; Sakamoto et al., 2018; Numano et al., 2019; Abdelgied et al., 2019; Chernova et al., 2017; Muller et al., 2009; Nagai et al., 2011; Nagai et al., 2013; Porter et al., 2013; Kasai et al., 2015; McKinney et al., 2009; Umeda et al., 2013; Kasai et al., 2014; Porter et al., 2013; Fortini et al., 2020; Mercer et al., 2013a; Kasai et al., 2015; Mercer et al., 2013b; Kasai et al., 2016; Xu et al., 2014; Morimoto et al., 2012; Oyabu et al., 2011; Shinohara et al., 2016; Murphy et al., 2012a; Ma-Hock et al., 2009; Muller et al., 2009; Chen et al., 2012; Xu et al., 2014; Liao et al., 2018; Poland et al., 2008; Ma-Hock et al., 2009; Zhu et al., 2016; Cui et al., 2014; Kadariya et al., 2016; Boyles et al., 2015; Palomäki et al., 2011; Lee et al., 2018; Chortarea et al., 2018; Murphy et al., 2012b; Hindman and Ma, 2019; Arnoldussen et al., 2015; Sanchez et al., 2011; Kabadi et al., 2019; Muller et al., 2005; Palomäki et al., 2015; Xu et al., 2012).

MWCNT	Mesothelioma categorization	Deposition in the distal lung/translocation to the pleural cavity	Dissolution/ Biopersistence	Fibre length >5µm	Rigid, needle-like morphology	Frustrated Phagocytosis	IATA outcome
Mitsui-7	**Mesothelioma-positive** Takagi 2008 Sakamoto 2009 Nagai 2011 Takagi 2012 Huaux 2016 Sakamoto 2018 Numano 2019 Abdelgied 2019	**DN: YES (Tier 2)** MMAD measured from aerosolized sample < 4µm.[30,47,110–112] **DN: YES (Tier 3)** Alveolar deposition measured in inhalation studies.[30,45,47,111] Translocation to the pleural observed (additional supporting evidence).[46,49]	**DN: YES (Tier1)** Predicted to be biodurable based on pristine carbon chemistry **DN: YES (Tier3)** Half-life *in vivo* > 60 days.[45]	**DN: YES (Tier 2)** Size profile measured from aerosolized samples- fibres > 5µm length identified.[47,112,113]	**DN: YES (Tier3)** Classified Mitsui-7 as 'biologically stiff' when exposed to the compressive forces of phagolysosomal membrane based on Euler buckling theory.[36]	**DN: YES (Tier1)** Significant IL-1β and CathepsinB release measured from macrophages in vitro, confirmed activation of NALP3 inflammasome.[25,26,36,38,63,98,114–117] **DN: YES (Tier2)** 3D macrophage granuloma formation after chronic in vitro exposure.[62,64]	**Accept grouping hypothesis** Sufficient information available at minimum Tier 2 for each DN
SD1	**Mesothelioma-positive** Sakamoto 2018	**DN: Deposition Not addressed** Translocation to the pleural observed (additional supporting evidence).[118]	**DN: YES (Tier1)** Predicted to be biodurable based on pristine carbon chemistry	**DN: YES (Tier 1)** Additional confirmation of fibres > 5µm from MWCNT suspension.[118,119]	**DN: YES (Tier1)** Diameter: 150nm[114]	**DN: YES (Tier 1)** Significant IL-1β release measured from macrophages in vitro, confirmed activation of NALP3 inflammasome.[114]	**Provisionally Accept grouping hypothesis** Remaining data gap: No information available on D_{ae}/MMAD to predict deposition.
N-CNT	**Mesothelioma-positive** Suzui 2016 *Additional studies used same bulk material but method of preparation or handling may affect integration of results with mesothelioma studies.	**DN: YES (Tier 2)** MMAD measured from aerosolized sample < 4µm.[120,121] **DN: YES (Tier 3)** Alveolar deposition measured in inhalation studies[120]* Translocation to the pleural observed (additional supporting evidence).[122]	**DN: YES (Tier1)** Predicted to be biodurable based on pristine carbon chemistry **DN: YES (Tier 3)** Half-life *in vivo* > 60 days: Lung burden was determined at 3d, 1 month and 3 months post exposure. Half-life after inhalation 51-54 days.[120] *short fibre preparation 30% of administrated MWCNTs were cleared by bronchial ciliary motion within 24 h of intratracheal administration. The pulmonary burden did not subsequently decrease significantly over time for up to 364 days after instillation.[123]	**DN: YES (Tier 2)** Size profile measured from aerosolized samples- fibres > 5µm length.[120]	**DN: YES (Tier1)**	**DN: Not reported**	**Provisionally Accept grouping hypothesis** Uncertainty over relevance of inhalation and biopersistence study as a shorter fibre preparation was used (Oyabu *et al* 2011, Morimoto *et al* 2011) Remaining data gap: Frustrated phagocytosis
NTlong	**Mesothelioma-positive** Chernova 2017	**DN: Deposition Not addressed** Translocation to the pleural observed (additional supporting evidence).[48]	**DN: YES (Tier1)** Predicted to be biodurable based on pristine carbon chemistry	**DN: YES (Tier1)** Proportion of fibres > 5µm not reported however 84.26% > 15µm Mean: 36µm[50]	**DN: YES (Tier1)** Mean: 165.02 ±4.68nm[50]	**DN: YES (Tier 1)** Significant IL-1β release measured from macrophages in vitro, confirmed activation of NALP3 inflammasome.[98]	**Provisionally Accept grouping hypothesis** Remaining data gap: No information available on D_{ae}/MMAD to predict deposition.
MWCNT+	**Mesothelioma-negative** Muller 2009	**DN: YES (Tier2)** MMAD measured from aerosolized sample.[41] **DN: YES (Tier3)** Alveolar deposition modelled and confirmed by visualization of MWCNT in the alveolar region of the lungs in inhalation studies.[41]	**DN: YES (Tier1)** Predicted to be biodurable based on pristine carbon chemistry **DN: NO (Tier3)** Half-life *in vivo* < 60 days: 78.4%±12.4 of initial burden recovered after Day 28, 36%±13.2 recovered after 60 days.[42]	**DN: NO (Tier 2)** No evidence of individual fibres or fibrous structures (AR>3:1) in aerosol. 'Mainly consisted of agglomerates of a few hundred nm to µms in diameter, with hairy surface consisting of numerous ends of MWCNT'[41]	**DN: NO (Tier 1)** Diameter: 5-15nm[41]	**DN: NO (Tier 1)** No significant IL-1β release measured from macrophages in vitro.[63] Dose-dependent cytotoxicity (LDH release) and significant increase in TNFα mRNA after 6hrs i and significant TNFα release after 24 hours incubation with macrophages (additional relevant information).[124]	**Reject grouping hypothesis** MWCNT does not meet the criteria for length or rigidity. Cytotoxicity and reactivity likely related to alternative MoA.
NTtng1	**Mesothelioma-negative** Nagai 2011 Nagai 2013 Sakamoto 2018	**DN: Deposition Not addressed** No evidence of translocation to the pleural cavity after TIPS in tissue sections visualized by light microscopy or SEM (Tier 3)(additional supporting evidence).[118]	**DN: YES (Tier1)** Predicted to be biodurable based on pristine carbon chemistry	**DN: NO (Tier 1)** 0.5-2µm from manufacturers Not measurable by authors due to highly tangled nature	**DN: NO (Tier 1)** 15nm (From manufacturer) Non-rigid nature of MWCNT confirmed by TEM and light microscopy images of highly tangled nature of MWCNT	**DN: NO (Tier 1)** Increase in IL-1β release but it is x2000 less potent than Mitsui-7 or SD1.[114]	**Reject grouping hypothesis** MWCNT does not meet the criteria for length, rigidity or frustrated phagocytosis.

	negative Nagai 2011 Nagai 2013 Sakamoto 2018	**addressed** No evidence of translocation to the pleural cavity after TIPS in tissue sections visualized by light microscopy or SEM (Tier 3)(additional supporting evidence).[118]	Predicted to be biodurable based on pristine carbon chemistry	0.5-2µm from manufacturers Not measurable by authors due to highly tangled nature	15nm (From manufacturer) Non-rigid nature of MWCNT confirmed by TEM and light microscopy images of highly tangled nature of MWCNT	Increase in IL-1β release but it is x2000 less potent than Mitsui-7 or SD1.[114]	MWCNT does not meet the criteria for length, rigidity or frustrated phagocytosis.

Table 7
Evaluation for potential impact of additional descriptors not included in the IATA on mesothelioma development. Mesothelioma-positive MWCNT are shaded in green, mesothelioma-negative MWCNT are shaded in red. Data not reported (NR) shaded in grey.

Purity %		Fe content %		Ni content %		D/G ratio	
SD1	99.9	WL-CNT	5.9	MWCNT D	1.5	SD2	1.5
MWCNT B	98.7	T-CNT	4.86	MWCNT C	0.27	MWCNT A	1.3
N-CNT	98	SD2	1.1	MWCNT A	0.19	MWCNT B	1.3
MWCNT A	97.62	NTlong	0.84	WS-CNT	0.189	MWCNT C	1.3
Mitsui-7	95	MWCNT+	0.49	MWCNT B	0.01	MWCNT D	1.3
MWCNT+	95	Mitsui-7	0.35	WL-CNT	0.007	MWCNT+	1.16
SD2	95	N-CNT	0.046	Mitsui-7	0.001	Mitsui-7	0.09
WS-CNT	95	WS-CNT	0.02	NTlong	0.001	SD1	NR
MWCNT C	94.79	SD1	0.002	T-CNT	0.001	N-CNT	NR
MWCNT D	94.72	MWCNT A	NR	MWCNT+	NR	NTlong	NR
WL-CNT	93	MWCNT B	NR	SD1	NR	NT50b	NR
T-CNT	85	MWCNT C	NR	SD2	NR	NT145	NR
NTlong	NR	MWCNT D	NR	N-CNT	NR	WL-CNT	NR
NT50b	NR	NT50b	NR	NT50b	NR	WS-CNT	NR
NT145	NR	NT145	NR	NT145	NR	T-CNT	NR

known drivers of fibre toxicity leading to mesothelioma development, and then substantiated through application of an IATA. This hypothesis-driven approach facilitates, *via* the IATA, the identification of HARNs which pose a mesothelioma hazard and directs the assessment of similarity between selected HARNs to support the formation of a group.

Evidence-based grouping of HARNs is timely in order to support risk assessment and risk decision making of HARNs. Currently the rigid, needle-like MWCNT, Mitsui-7, is classified by IARC as a 'possible human carcinogen', however this classification cannot be extended to other MWCNT due to insufficient evidence of *in vivo* carcinogenicity required for each individual MWCNT (Grosse et al., 2014). Conversely ChemSec, an independent non-profit organisation that advocates for substitution of toxic chemicals to safer alternatives, has included all forms of CNT on their SIN ('substitute it now') list of chemicals they believe should be restricted or banned in the EU, citing a lack of evidence to 'justify where to draw a line between hazardous and less hazardous carbon nanotubes' (Hansen and Lennquist, 2020). The ChemSec approach groups CNT based on chemical composition alone, and does not recognize varying properties that may elicit distinct biological outcomes *in vitro* and *in vivo* (Fadeel and Kostarelos, 2020).

This approach of using well-substantiated, hypothesis-driven grouping may be used to support the waiving of extensive *in vivo* (tier 3) safety testing of materials for purposes such as regulatory hazard categorization or SbD decision making. The structured format of the IATA decision tree highlights where evidence required to support a grouping decision may be lacking, allowing data gaps to be prioritised for targeted testing using tier 1 and tier 2 methods, and areas of uncertainty to be transparently addressed. Overall the adoption of the GRACIOUS Framework for grouping HARNs will address the currently unmet need for a robust and streamlined hazard assessment of these novel, but potentially pathogenic, fibrous materials.

The literature based case study used to test the performance of the IATA demonstrated the IATA DNs were stringent enough to differentiate between mesothelioma-positive and mesothelioma-negative MWCNT, and therefore can be used to support the formation of groups based on distinct biological outcomes. Further similarity assessment between the group members according to the IATA DNs could be used to strengthen the mechanistic argument for read-across between group members, to minimise the burden of carcinogenicity testing. Defining the acceptable limits of similarity for each of the HARN IATA DNs represents the next step in the development of the IATA. When applied to a comparison of HARNs within the proposed group, these limits will enable an assessment of the relative similarity between the HARNs which can support the argument for interpolation of hazard data between group members.

Here we have presented the hypothesis for grouping HARN on the basis of the potential hazard posed to the mesothelium, which may be distinct, albeit often overlapping, with the hazard posed by HARN and fibres within the lungs (fibrosis and lung tumours). In addition, a HARN may trigger multiple MoA in the lung which result in a range of pathological adverse effects. For example, effects could be driven by surface reactivity, metal contamination or particle overload (Wang et al., 2017). This means that the user may need to consider more than one hypothesis and IATA, especially if the hypothesis for mesothelioma hazard is rejected. Additional pre-defined hypothesis are currently under development within the GRACIOUS project which will cover different MoA and different routes of exposure.

The HARN IATA presented here has been developed based on 'simple' HARNs which may not reflect industrially-relevant, more complex forms and mixtures. However as demonstrated by the extensive evidence-base underpinning the grouping hypothesis and IATA, the key criteria for determining a fibre-like hazard are robust, and therefore likely to also hold true for novel materials and mixtures. The inclusion of such materials is considered out with the scope of the current project however in future the HARN IATA may be used as a robust foundation for an adapted testing strategy, appropriate to assess more complex and novel materials and mixtures.

The HARN hypothesis and IATA are being integrated into the GRACIOUS Framework software blueprint, currently under development and testing by stakeholders. By linking to NM databases (*e.g.* eNanoMapper(Jeliazkova et al., 2015)) an open-access blueprint will

facilitate the rapid identification of potential group members or putative source materials providing a user-friendly interface to facilitate the use of the IATA to support grouping and read-across (Stone et al., 2020). The MWCNT case study employed here, to manually test the IATA performance, required some level of expert opinion to justify the formation of mesothelioma-positive groups, due to the limitations and quality of data available in the literature. In future as the IATA are adopted and utilized, the NM databases will be populated with the required information specified by the IATA which will help to increase the automation of the grouping process though use of the blueprint software.

Here we have demonstrated the practical application of a GRACIOUS IATA supporting an evidence-based grouping hypothesis for HARNs in relation to their structural similarity to pathogenic asbestos fibres and the associated potential to pose a mesothelioma hazard. This IATA illustrates how the mechanistic links between PC characteristics, such as size and shape, and factors such as biopersistence and toxicokinetics can be integrated and evidenced to form a well-substantiated grouping hypothesis. Furthermore we demonstrated how the implementation of the IATA in tiers of testing with increasing specificity and complexity, will identify/generate the evidence required to test the hypothesis, as well as reduce, refine and replace the need for animal testing. This will result in well-substantiated grouping of HARNs for a number of applications spanning the fields of regulation, innovation, industry and academia.

Declaration of Competing Interest

The authors declare that they have no known competing financial interests or personal relationships that could have appeared to influence the work reported in this paper.

Acknowledgements

The GRACIOUS project was supported by the European Commission Horizon 2020 programme, Grant Agreement No. 760840.

References

Abdelgied, M., et al., 2019. Carcinogenic effect of potassium octatitanate (POT) fibers in the lung and pleura of male Fischer 344 rats after intrapulmonary administration. Part. Fibre Toxicol. 16, 34.
Arnoldussen, Y.J., et al., 2015. Involvement of IL-1 genes in the cellular responses to carbon nanotube exposure. Cytokine 73, 128–137.
Asgharian, B., Yu, C.P., 1989. Deposition of fibers in the rat lung. J. Aerosol Sci. 20, 355–366.
Bello, D., et al., 2009. Exposure to nanoscale particles and fibers during machining of hybrid advanced composites containing carbon nanotubes. J. Nanopart. Res. 11, 231–249.
Bernstein, D.M., et al., 1997. The biopersistence of fibres following inhalation and intratracheal instillation exposure. Ann. Occup. Hyg. 41, 224–230.
Bitounis, D., Pyrgiotakis, G., Bousfield, D., Demokritou, P., 2019. Dispersion preparation, characterization, and dosimetric analysis of cellulose nano-fibrils and nano-crystals: implications for cellular toxicological studies. NanoImpact 15, 100171.
Boulanger, G., et al., 2014. Quantification of short and long asbestos fibers to assess asbestos exposure: a review of fiber size toxicity. Environ. Health 13, 59.
Boyles, M.S.P., et al., 2015. Multi-walled carbon nanotube induced frustrated phagocytosis, cytotoxicity and pro-inflammatory conditions in macrophages are length dependent and greater than that of asbestos. Toxicol. Vitr. 29, 1513–1528.
Broz, P., Dixit, V.M., 2016. Inflammasomes: mechanism of assembly, regulation and signalling. Nat. Rev. Immunol. 16, 407–420.
BSI, 1993. BS EN 481:1993, BS 6069–3.5:1993 Workplace atmospheres. In: Size Fraction Definitions for Measurement of Airborne Particles. European Committee for Standardization.
BSI, 2019. BS EN 17199–1:2019 Workplace exposure. Measurement of dustiness of bulk materials that contain or release respirable NOAA and other respirable particles. In: Requirements and Choice of Test Methods. BSI Standards Limited.
Cena, L.G., Peters, T.M., 2011. Characterization and control of airborne particles emitted during production of epoxy/carbon nanotube nanocomposites. J. Occup. Environ. Hyg. 8, 86–92.
Chen, B.T., et al., 2012. Multi-walled carbon nanotubes: sampling criteria and aerosol characterization. Inhal. Toxicol. 24, 798–820.
Chernova, T., et al., 2017. Long-fiber carbon nanotubes replicate asbestos-induced mesothelioma with disruption of the tumor suppressor gene Cdkn2a (Ink4a/Arf). Curr. Biol. 27, 3302–3314.e6.
Chortarea, S., et al., 2018. Profibrotic activity of multiwalled carbon nanotubes upon prolonged exposures in different human lung cell types. Appl. Vitr. Toxicol. 5, 47–61.
Commission, E, 2018. *Commission Regulation (EU)* 2018/*1881 of 3 December 2018 amending Regulation (EC) No 1907/2006 of the European Parliament and of the Council on the Registration, Evaluation, Authorisation and Restriction of Chemicals (REACH) as regards Annexes I, III,VI, V*.
Cui, H., et al., 2014. High-temperature calcined fullerene nanowhiskers as well as long needle-like multi-wall carbon nanotubes have abilities to induce NLRP3-mediated IL-1β secretion. Biochem. Biophys. Res. Commun. 452, 593–599.
Dahm, M.M., Evans, D.E., Schubauer-Berigan, M.K., Birch, M.E., Fernback, J.E., 2012. Occupational exposure assessment in carbon nanotube and Nanofiber primary and secondary manufacturers. Ann. Occup. Hyg. 56, 542–556.
David, Bernstein, Juan, Riego, 1999. Methods for the Determination of the Hazardous Properties for Human Health of Man Made Mineral Fibres (MMMF). http://publications.jrc.ec.europa.eu/repository/handle/JRC18422.
Davis, J.M., et al., 1986. The pathogenicity of long versus short fibre samples of amosite asbestos administered to rats by inhalation and intraperitoneal injection. Br. J. Exp. Pathol. 67, 415–430.
DeLoid, G.M., et al., 2015. Advanced computational modeling for in vitro nanomaterial dosimetry. Part. Fibre Toxicol. 12, 32.
Donaldson, K., Murphy, F.A., Duffin, R., Poland, C.A., 2010. Asbestos, carbon nanotubes and the pleural mesothelium: a review of the hypothesis regarding the role of long fibre retention in the parietal pleura, inflammation and mesothelioma. Part. Fibre Toxicol. 7, 5.
Dostert, C., et al., 2008. Innate immune activation through Nalp3 inflammasome sensing of asbestos and silica. Science (80-.) 320, 674 LP – 677.
Dresselhaus, M.S., Jorio, A., Souza Filho, A.G., Saito, R., 2010. Defect characterization in graphene and carbon nanotubes using Raman spectroscopy. Philos. Trans. R. Soc. A Math. Phys. Eng. Sci. 368, 5355–5377.
Duke, K.S., et al., 2017. STAT1-dependent and -independent pulmonary allergic and fibrogenic responses in mice after exposure to tangled versus rod-like multi-walled carbon nanotubes. Part. Fibre Toxicol. 14, 26.
European Chemicals Agency, 2008. Guidance on information requirements and chemical safety assessment Appendix R.6 Guidance on QSARs and Grouping of Chemicals. https://echa.europa.eu/guidance-documents/guidance-on-information-requirements-and-chemical-safety-assessment.
European Chemicals Agency, 2017. Read-Across Assessment Framework (RAAF). https://doi.org/10.2823/619212.
European Chemicals Agency, 2019a. Appendix R.6-1 for nanoforms applicable to the Guidance on QSARs and grouping of Chemicals. https://doi.org/10.2823/273911. https://echa.europa.eu/documents/10162/2324906/appendix_r6_nanomaterials_en.pdf/71ad76f0-ab4c-fb04-acba-074cf045eaaa?t=1575294955659.
European Chemicals Agency, 2019b. Appendix for nanoforms applicable to the Guidance on Registration and Substance Identification. https://doi.org/10.2823/832485. https://echa.europa.eu/documents/10162/23047722/appendix_nanoforms_msc_rac_forum_eng.pdf/a68660cd-4cf2-7437-cf0b-56e628a48d76.
Fadeel, B., Kostarelos, K., 2020. Grouping all carbon nanotubes into a single substance category is scientifically unjustified. Nat. Nanotechnol. 15, 164.
Fortini, R., et al., 2020. Measurement of flexural rigidity of multi-walled carbon nanotubes by dynamic scanning electron microscopy. Fibers 8.
Gerloff, K., et al., 2017. The adverse outcome pathway approach in nanotoxicology. Comput. Toxicol. 1, 3–11.
Grosse, Y., et al., 2014. Carcinogenicity of fluoro-edenite, silicon carbide fibres and whiskers, and carbon nanotubes. Lancet. Oncol. 15, 1427–1428.
Gualtieri, A.F., Pollastri, S., Bursi Gandolfi, N., Gualtieri, M.L., 2018. In vitro acellular dissolution of mineral fibres: a comparative study. Sci. Rep. 8, 7071.
Halappanavar, S., et al., 2020. Adverse outcome pathways as a tool for the design of testing strategies to support the safety assessment of emerging advanced materials at the nanoscale. Part. Fibre Toxicol. 17, 16.
Hamilton, R.F., et al., 2009. Particle length-dependent titanium dioxide nanomaterials toxicity and bioactivity. Part. Fibre Toxicol. 6, 35.
Han, J.H., et al., 2008. Monitoring multiwalled carbon nanotube exposure in carbon nanotube research facility. Inhal. Toxicol. 20, 741–749.
Hansen, S.F., Lennquist, A., 2020. Carbon nanotubes added to the SIN list as a nanomaterial of very high concern. Nat. Nanotechnol. 15, 3–4.
Hinderliter, P.M., et al., 2010. ISDD: a computational model of particle sedimentation, diffusion and target cell dosimetry for in vitro toxicity studies. Part. Fibre Toxicol. 7, 36.
Hindman, B., Ma, Q., 2019. Carbon nanotubes and crystalline silica stimulate robust ROS production, inflammasome activation, and IL-1β secretion in macrophages to induce myofibroblast transformation. Arch. Toxicol. 93, 887–907.
Huaux, F., et al., 2016. Mesothelioma response to carbon nanotubes is associated with an early and selective accumulation of immunosuppressive monocytic cells. Part. Fibre Toxicol. 13, 46.
ISO, 2017. ISO/TR 19057:2017 Nanotechnologies. Use and application of acellular in vitro tests and methodologies to assess nanomaterial biodurability. ISO.
Jeliazkova, N., et al., 2015. The eNanoMapper database for nanomaterial safety information. Beilstein J. Nanotechnol. 6, 1609–1634.
Ji, Z., et al., 2012. Designed synthesis of CeO2 nanorods and nanowires for studying toxicological effects of high aspect ratio nanomaterials. ACS Nano 6, 5366–5380.
Kabadi, P.K., et al., 2019. A novel human 3D lung microtissue model for nanoparticle-induced cell-matrix alterations. Part. Fibre Toxicol. 16, 15.
Kadariya, Y., et al., 2016. Inflammation-related IL1β/IL1R signaling promotes the development of Asbestos-induced malignant mesothelioma. Cancer Prev. Res. (Phila.) 9 (406–414).

Kane, A.B., Hurt, R.H., Gao, H., 2018. The asbestos-carbon nanotube analogy: an update. Toxicol. Appl. Pharmacol. 361, 68–80.
Kasai, T., et al., 2014. Development of a new multi-walled carbon nanotube (MWCNT) aerosol generation and exposure system and confirmation of suitability for conducting a single-exposure inhalation study of MWCNT in rats. Nanotoxicology 8, 169–178.
Kasai, T., et al., 2015. Thirteen-week study of toxicity of fiber-like multi-walled carbon nanotubes with whole-body inhalation exposure in rats. Nanotoxicology 9, 413–422.
Kasai, T., et al., 2016. Lung carcinogenicity of inhaled multi-walled carbon nanotube in rats. Part. Fibre Toxicol. 13, 53.
Koltermann-Jülly, J., et al., 2018. Abiotic dissolution rates of 24 (nano)forms of 6 substances compared to macrophage-assisted dissolution and in vivo pulmonary clearance: grouping by biodissolution and transformation. NanoImpact 12, 29–41.
Krombach, F., et al., 1997. Cell size of alveolar macrophages: an interspecies comparison. Environ. Health Perspect. 105, 1261–1263.
Kuijpers, E., et al., 2016. Occupational exposure to multi-walled carbon nanotubes during commercial production synthesis and handling. Ann. Occup. Hyg. 60, 305–317.
Lee, J.H., et al., 2010. Exposure assessment of carbon nanotube manufacturing workplaces. Inhal. Toxicol. 22, 369–381.
Lee, D.-K., et al., 2018. Threshold rigidity values for the asbestos-like pathogenicity of high-aspect-ratio carbon nanotubes in a mouse pleural inflammation model. ACS Nano 12, 10867–10879.
Lehmann, S.G., et al., 2019. Crumpling of silver nanowires by endolysosomes strongly reduces toxicity. Proc. Natl. Acad. Sci. 116, 14893 LP – 14898.
Liao, D., et al., 2018. Persistent pleural lesions and inflammation by pulmonary exposure of multiwalled carbon nanotubes. Chem. Res. Toxicol. 31, 1025–1031.
Lippmann, M., 1988. Asbestos exposure indices. Environ. Res. 46, 86–106.
Lippmann, M., 2014. Toxicological and epidemiological studies on effects of airborne fibers: coherence and public health implications. Crit. Rev. Toxicol. 44, 643–695.
Liu, R., et al., 2015. Evaluation of toxicity ranking for metal oxide nanoparticles via an in vitro Dosimetry model. ACS Nano 9, 9303–9313.
Luoto, K., Holopainen, M., Savolainen, K., 1995. Durability of man-made vitreous fibres as assessed by dissolution of silicon, iron and aluminium in rat alveolar macrophages. Ann. Occup. Hyg. 39, 855–867.
Ma-Hock, L., et al., 2009. Inhalation toxicity of multiwall carbon nanotubes in rats exposed for 3 months. Toxicol. Sci. 112, 468–481.
Maxim, L.D., Boymel, P., Chase, G.R., Bernstein, D.M., 2002. Indices of Fiber biopersistence and carcinogen classification for synthetic vitreous fibers (SVFs). Regul. Toxicol. Pharmacol. 35, 357–378.
Maynard, A.D., et al., 2004. Exposure to carbon nanotube material: aerosol release during the handling of unrefined single-walled carbon nanotube material. J. Toxicol. Environ. Heal. Part A 67, 87–107.
McKinney, W., Chen, B., Frazer, D., 2009. Computer controlled multi-walled carbon nanotube inhalation exposure system. Inhal. Toxicol. 21, 1053–1061.
Mech, A., Rauscher, H., Babick, F., Hodoroaba, V., Ghanem, A., Wohlleben, W., Hans, Marvin, Weigel, S., Brungel, R., Friedrich, C.M., Kirsten, Rasmussen, Loeschner, K., Gilliland, D., 2020. The NanoDefine Methods Manual. https://publications.jrc.ec.europa.eu/repository/handle/JRC117501.
Mercer, R.R., et al., 2013a. Distribution and fibrotic response following inhalation exposure to multi-walled carbon nanotubes. Part. Fibre Toxicol. 10, 33.
Mercer, R.R., et al., 2013b. Extrapulmonary transport of MWCNT following inhalation exposure. Part. Fibre Toxicol. 10, 38.
Miller, F.J., Asgharian, B., Schroeter, J.D., Price, O., 2016. Improvements and additions to the multiple path particle Dosimetry model. J. Aerosol Sci. 99, 14–26.
Miserocchi, G., Sancini, G., Mantegazza, F., Chiappino, G., 2008. Translocation pathways for inhaled asbestos fibers. Environ. Health 7, 4.
Moalli, P.A., MacDonald, J.L., Goodglick, L.A., Kane, A.B., 1987. Acute injury and regeneration of the mesothelium in response to asbestos fibers. Am. J. Pathol. 128, 426–445.
Morimoto, Y., et al., 2012. Pulmonary toxicity of well-dispersed multi-wall carbon nanotubes following inhalation and intratracheal instillation. Nanotoxicology 6, 587–599.
Mossman, B.T., Churg, A., 1998. Mechanisms in the pathogenesis of asbestosis and silicosis. Am. J. Respir. Crit. Care Med. 157, 1666–1680.
Muller, J., et al., 2005. Respiratory toxicity of multi-wall carbon nanotubes. Toxicol. Appl. Pharmacol. 207, 221–231.
Muller, J., et al., 2008. Structural defects play a major role in the acute lung toxicity of multiwall carbon nanotubes: toxicological aspects. Chem. Res. Toxicol. 21, 1698–1705.
Muller, J., et al., 2009. Absence of carcinogenic response to multiwall carbon nanotubes in a 2-year bioassay in the peritoneal cavity of the rat. Toxicol. Sci. 110, 442–448.
Murphy, F.A., et al., 2011. Length-dependent retention of carbon nanotubes in the pleural space of mice initiates sustained inflammation and progressive fibrosis on the parietal pleura. Am. J. Pathol. 178, 2587–2600.
Murphy, F.A., Poland, C.A., Duffin, R., Donaldson, K., 2012a. Length-dependent pleural inflammation and parietal pleural responses after deposition of carbon nanotubes in the pulmonary airspaces of mice. Nanotoxicology 7, 1157–1167.
Murphy, F.A., Schinwald, A., Poland, C.A., Donaldson, K., 2012b. The mechanism of pleural inflammation by long carbon nanotubes: interaction of long fibres with macrophages stimulates them to amplify pro-inflammatory responses in mesothelial cells. Part. Fibre Toxicol. 9, 8.
Nagai, H., et al., 2011. Diameter and rigidity of multiwalled carbon nanotubes are critical factors in mesothelial injury and carcinogenesis. Proc. Natl. Acad. Sci. 108. E1330 LP-E1338.
Nagai, H., et al., 2013. Intraperitoneal administration of tangled multiwalled carbon nanotubes of 15 nm in diameter does not induce mesothelial carcinogenesis in rats. Pathol. Int. 63, 457–462.
Nguea, H., de Reydellet, A., Le Faou, A., Zaiou, M., Rihn, B., 2008. Macrophage culture as a suitable paradigm for evaluation of synthetic vitreous fibers. Crit. Rev. Toxicol. 38, 675–695.
Noonan, C.W., 2017. Environmental asbestos exposure and risk of mesothelioma. Ann. Transl. Med. 5, 234.
Numano, T., et al., 2019. MWCNT-7 administered to the lung by intratracheal instillation induces development of pleural mesothelioma in F344 rats. Cancer Sci. 110, 2485–2492.
OECD, 2017. Guidance Document on the Reporting of Defined Approaches to be Used Within Integrated Approaches to Testing and Assessment. OECD. https://doi.org/10.1787/9789264274822-en.
OECD, 2018a. Test No. 412: Subacute Inhalation Toxicity: 28-Day Study. OECD. https://doi.org/10.1787/9789264070783-en.
OECD, 2018b. Test No. 413: Subchronic Inhalation Toxicity: 90-day Study. OECD. https://doi.org/10.1787/9789264070806-en.
Oyabu, T., et al., 2011. Biopersistence of inhaled MWCNT in rat lungs in a 4-week well-characterized exposure. Inhal. Toxicol. 23, 784–791.
Palomäki, J., et al., 2011. Long, needle-like carbon nanotubes and Asbestos activate the NLRP3 Inflammasome through a similar mechanism. ACS Nano 5, 6861–6870.
Palomäki, J., et al., 2015. A secretomics analysis reveals major differences in the macrophage responses towards different types of carbon nanotubes. Nanotoxicology 9, 719–728.
Park, M.V.D.Z., et al., 2018. Development of a systematic method to assess similarity between nanomaterials for human hazard evaluation purposes – lessons learnt. Nanotoxicology 12, 652–676.
Poland, C.A., et al., 2008. Carbon nanotubes introduced into the abdominal cavity of mice show asbestos-like pathogenicity in a pilot study. Nat. Nanotechnol. 3, 423–428.
Porter, D.W., et al., 2013. Acute pulmonary dose-responses to inhaled multi-walled carbon nanotubes. Nanotoxicology 7, 1179–1194.
Price, S.R., Kinnear, C., Balog, S., 2019. Particokinetics and in vitro dose of high aspect ratio nanoparticles. Nanoscale 11, 5209–5214.
Rittinghausen, S., et al., 2014. The carcinogenic effect of various multi-walled carbon nanotubes (MWCNTs) after intraperitoneal injection in rats. Part. Fibre Toxicol. 11, 59.
Ryman-Rasmussen, J.P., et al., 2009. Inhaled carbon nanotubes reach the subpleural tissue in mice. Nat. Nanotechnol. 4, 747–751.
Sakamoto, Y., et al., 2009. Induction of mesothelioma by a single intrascrotal administration of multi-wall carbon nanotube in intact male Fischer 344 rats. J. Toxicol. Sci. 34, 65–76.
Sakamoto, Y., et al., 2018. Comparative study for carcinogenicity of 7 different multi-wall carbon nanotubes with different physicochemical characteristics by a single intraperitoneal injection in male Fischer 344 rats. J. Toxicol. Sci. 43, 587–600.
Saleh, D.M., et al., 2020. Comparative carcinogenicity study of a thick, straight-type and a thin, tangled-type multi-walled carbon nanotube administered by intra-tracheal instillation in the rat. Part. Fibre Toxicol. 17, 48.
Sanchez, V.C., Weston, P., Yan, A., Hurt, R.H., Kane, A.B., 2011. A 3-dimensional in vitro model of epithelioid granulomas induced by high aspect ratio nanomaterials. Part. Fibre Toxicol. 8, 17.
Sayan, M., Mossman, B.T., 2016. The NLRP3 inflammasome in pathogenic particle and fibre-associated lung inflammation and diseases. Part. Fibre Toxicol. 13, 51.
Schinwald, A., Donaldson, K., 2012. Use of back-scatter electron signals to visualise cell/nanowires interactions in vitro and in vivo; frustrated phagocytosis of long fibres in macrophages and compartmentalisation in mesothelial cells in vivo. Part. Fibre Toxicol. 9, 34.
Schinwald, A., et al., 2012. The threshold length for Fiber-induced acute pleural inflammation: shedding light on the early events in Asbestos-induced mesothelioma. Toxicol. Sci. 128, 461–470.
Shinohara, N., et al., 2016. Long-term retention of pristine multi-walled carbon nanotubes in rat lungs after intratracheal instillation. J. Appl. Toxicol. 36, 501–509.
Stanton, M.F., et al., 1977. Carcinogenicity of fibrous glass: pleural response in the rat in relation to fiber dimension. JNCI J. Natl. Cancer Inst. 58, 587–603.
Stanton, M.F., et al., 1981. Relation of particle dimension to carcinogenicity in amphibole asbestoses and other fibrous minerals. J. Natl. Cancer Inst. 67, 965–975.
Stayner, L., Welch, L.S., Lemen, R., 2013. The worldwide pandemic of Asbestos-related diseases. Annu. Rev. Public Health 34, 205–216.
Stone, V., et al., 2014. ITS-NANO - Prioritising nanosafety research to develop a stakeholder driven intelligent testing strategy. Part. Fibre Toxicol. 11, 9.
Stone, V., et al., 2020. A framework for grouping and read-across of nanomaterials-supporting innovation and risk assessment. Nano Today 35, 100941.
Suzui, M., et al., 2016. Multiwalled carbon nanotubes intratracheally instilled into the rat lung induce development of pleural malignant mesothelioma and lung tumors. Cancer Sci. 107, 924–935.
Takagi, A., et al., 2008. Induction of mesothelioma in p53+/− mouse by intraperitoneal application of multi-wall carbon nanotube. J. Toxicol. Sci. 33, 105–116.
Takagi, A., Hirose, A., Futakuchi, M., Tsuda, H., Kanno, J., 2012. Dose-dependent mesothelioma induction by intraperitoneal administration of multi-wall carbon nanotubes in p53 heterozygous mice. Cancer Sci. 103, 1440–1444.
Thomas, D.G., et al., 2018. ISD3: a particokinetic model for predicting the combined effects of particle sedimentation, diffusion and dissolution on cellular dosimetry for in vitro systems. Part. Fibre Toxicol. 15, 6.

Tsai, C.S.-J., Hofmann, M., Hallock, M., Ellenbecker, M., Kong, J., 2015. Assessment of exhaust emissions from carbon nanotube production and particle collection by sampling filters. J. Air Waste Manage. Assoc. 65, 1376–1385.
Umeda, Y., et al., 2013. Two-week toxicity of multi-walled carbon nanotubes by whole-body inhalation exposure in rats. J. Toxicol. Pathol. 26, 131–140.
Varga, C., Szendi, K., 2010. Carbon nanotubes induce granulomas but not mesotheliomas. In Vivo (Brooklyn). 24 (153–156).
Villeneuve, D.L., et al., 2014. Adverse outcome pathway (AOP) development I: strategies and principles. Toxicol. Sci. 142, 312–320.
Wang, X., Sun, B., Liu, S., Xia, T., 2017. Structure activity relationships of engineered nanomaterials in inducing NLRP3 inflammasome activation and chronic lung fibrosis. NanoImpact 6, 99–108.
Wang, F., et al., 2019. Length and diameter-dependent phagocytosis and cytotoxicity of long silver nanowires in macrophages. Chemosphere 237, 124565.
Warheit, D.B., Reed, K.L., Stonehuerner, J.D., Ghio, A.J., Webb, T.R., 2006. Biodegradability of para-aramid respirable-sized fiber-shaped particulates (RFP) in human lung Cells1. Toxicol. Sci. 89, 296–303.
World Health Organisation, 1997. Determination of airborne fibre number concentrations: a recommended method, by phase-contrast optical microscopy (membrane filter method). World Health Organisation.
Xu, J., et al., 2012. Multi-walled carbon nanotubes translocate into the pleural cavity and induce visceral mesothelial proliferation in rats. Cancer Sci. 103, 2045–2050.
Xu, J., et al., 2014. Size- and shape-dependent pleural translocation, deposition, fibrogenesis, and mesothelial proliferation by multiwalled carbon nanotubes. Cancer Sci. 105, 763–769.
Zhu, W., et al., 2016. Nanomechanical mechanism for lipid bilayer damage induced by carbon nanotubes confined in intracellular vesicles. Proc. Natl. Acad. Sci. 113, 12374 LP – 12379.